

1 **Obstructive sleep apnea is associated with specific gut microbiota species and functions in**  
2 **the population-based Swedish CardioPulmonary bioImage Study (SCAPIS)**

3 Gabriel Baldanzi<sup>1</sup>, Sergi Sayols-Baixeras<sup>1,2</sup>, Jenny Theorell-Haglöw<sup>1,3</sup>, Koen F Dekkers<sup>1</sup>, Ulf  
4 Hammar<sup>1</sup>, Diem Nguyen<sup>1</sup>, Yi-Ting Lin<sup>1,4,5</sup>, Shafqat Ahmad<sup>1,6</sup>, Jacob Bak Holm<sup>7</sup>, Henrik Bjørn  
5 Nielsen<sup>7</sup>, Louise Brunkwall<sup>8</sup>, Christian Benedict<sup>9</sup>, Jonathan Cedernaes<sup>10,11</sup>, Sanna Koskiniemi<sup>12</sup>,  
6 Mia Phillipson<sup>11</sup>, Lars Lind<sup>13</sup>, Johan Sundström<sup>13,14</sup>, Göran Bergström<sup>15,16</sup>, Gunnar Engström<sup>8</sup>, J  
7 Gustav Smith<sup>17,18,19</sup>, Marju Orho-Melander<sup>8</sup>, Johan Ärnlöv<sup>4,20</sup>, Beatrice Kennedy<sup>1</sup>, Eva  
8 Lindberg<sup>3†</sup>, and Tove Fall<sup>1†\*</sup>.

9  
10 <sup>1</sup>Department of Medical Sciences, Molecular Epidemiology and Science for Life Laboratory,  
11 Uppsala University, Uppsala, Sweden;

12 <sup>2</sup>CIBER Cardiovascular diseases (CIBERCV), Instituto de Salud Carlos III, Madrid, Spain

13 <sup>3</sup>Department of Medical Sciences, Respiratory, Allergy and Sleep Research, Uppsala  
14 University, Uppsala, Sweden;

15 <sup>4</sup>Division of Family Medicine and Primary Care, Department of Neurobiology, Care Science and  
16 Society, Karolinska Institute, Huddinge, Sweden;

17 <sup>5</sup>Department of Family Medicine, Kaohsiung Medical University Hospital, Kaohsiung Medical  
18 University, Taiwan

19 <sup>6</sup>Preventive Medicine Division, Harvard Medical School, Brigham and Women's Hospital,  
20 Boston, United States

21 <sup>7</sup>Clinical Microbiomics A/S, Copenhagen, Denmark;

22 <sup>8</sup>Department of Clinical Sciences in Malmö, Lund University Diabetes Center, Lund University,  
23 Malmö, Sweden;

- 24 <sup>9</sup>Molecular Neuropharmacology (Sleep Science Lab), Department of Pharmaceutical  
25 Biosciences, Uppsala University, Uppsala, Sweden;
- 26 <sup>10</sup>Department of Medical Sciences, Transplantation and regenerative medicine, Uppsala  
27 University, Uppsala, Sweden;
- 28 <sup>11</sup>Department of Medical Cell Biology and Science for Life Laboratory, Uppsala University,  
29 Uppsala, Sweden;
- 30 <sup>12</sup>Department of Cell and Molecular Biology, Uppsala University, Uppsala, Sweden;
- 31 <sup>13</sup>Department of Medical Sciences, Clinical Epidemiology, Uppsala University, Uppsala,  
32 Sweden;
- 33 <sup>14</sup>The George Institute for Global Health, University of New South Wales, Sydney, Australia
- 34 <sup>15</sup>Department of Molecular and Clinical Medicine, Institute of Medicine, Sahlgrenska Academy,  
35 University of Gothenburg, Gothenburg, Sweden;
- 36 <sup>16</sup>Department of Clinical Physiology, Sahlgrenska University Hospital, Region Västra Götaland,  
37 Gothenburg, Sweden;
- 38 <sup>17</sup>The Wallenberg Laboratory/Department of Molecular and Clinical Medicine, Institute of  
39 Medicine, Gothenburg University and the Department of Cardiology, Sahlgrenska University  
40 Hospital, Gothenburg, Sweden;
- 41 <sup>18</sup>Department of Cardiology, Clinical Sciences, Lund University and Skåne University Hospital,  
42 Lund, Sweden;
- 43 <sup>19</sup>Wallenberg Center for Molecular Medicine and Lund University Diabetes Center, Lund  
44 University, Lund, Sweden;
- 45 <sup>20</sup>School of Health and Social Studies, Dalarna University, Falun, Sweden
- 46 \* Corresponding author

47 † Shared senior authorship.

48

49 Corresponding author:

50 Tove Fall, EpiHubben, Uppsala University

51 751 85 Uppsala, Sweden

52 Email: [tove.fall@medsci.uu.se](mailto:tove.fall@medsci.uu.se)

53

## 54 **Abstract**

55 Obstructive sleep apnea (OSA) is a common sleep-related breathing disorder. In animal models,  
56 OSA has been shown to alter the gut microbiota; however, little is known about such effects in  
57 humans. Here, we used respiratory polygraphy data from 3,570 individuals aged 50–64 from the  
58 Swedish CardioPulmonary bioImage Study (SCAPIS) and deep shotgun metagenomics to  
59 identify OSA-associated gut microbiota features. We found that OSA-related hypoxia parameters  
60 were associated with 128 bacterial species, including positive associations with *Blautia obeum*  
61 and *Collinsella aerofacines*. The latter was also associated with increased systolic blood pressure.  
62 Further, the cumulative time in hypoxia was associated with nine gut microbiota metabolic  
63 pathways, including propionate production from lactate, a biomarker of hypoxia. In conclusion,  
64 in this first large-scale study on gut microbiota alterations in OSA, we found that OSA-related  
65 hypoxia is associated with specific microbiota features. Our findings can direct future research  
66 on microbiota-mediated health effects of OSA.

67

## 68 **Introduction**

69 Obstructive sleep apnea (OSA) is characterized by upper airway collapse episodes during sleep  
70 resulting in complete cessation (apneas) or reduction (hypopneas) of air flow and consequent  
71 intermittent hypoxia<sup>1</sup>. It is estimated that OSA affects 5–36% of the adult population, depending  
72 on the country studied and the diagnostic criteria used. The increasing prevalence of OSA has  
73 been attributed to the increased longevity worldwide and the rising prevalence of obesity<sup>2</sup>, a  
74 well-described cause of OSA<sup>3</sup>. Although OSA has been prospectively associated with  
75 cardiovascular disease independent of BMI<sup>4,5</sup>, the mechanisms are not yet fully elucidated<sup>6</sup>.

76 The most commonly used clinical parameter of OSA severity is the apnea-hypopnea-  
77 index (AHI), which quantifies the number of apnea and hypopnea events per hour of sleep.  
78 However, AHI does not differentiate short apnea events with mild oxygen desaturation from  
79 prolonged events with severe hypoxia<sup>7</sup>. To quantify the time in hypoxia during sleep, the  
80 assessment for OSA often measures the percentage of the sleep time with oxygen saturation  
81 <90% (T90). The T90 parameter is a more reliable metric of nocturnal hypoxia intensity but  
82 not always associated with AHI<sup>8</sup>. Lastly, the oxygen desaturation index (ODI), which quantifies  
83 the number of oxygen desaturation events per hour of sleep<sup>9</sup>, is considered the most suitable  
84 parameter when the sole purpose is to measure intermittent hypoxia<sup>10</sup>. In sum, the three  
85 parameters are complementary to each other as they capture different dimensions of OSA.

86 The microbiota is a complex microbial community that interacts continuously with the  
87 host<sup>11</sup>. Studies of animal models of OSA have found that intermittent hypoxia and intermittent  
88 airway obstruction can produce substantial changes in the gut microbiota composition<sup>12–15</sup>. In  
89 turn, alterations of the gut microbiota induced by OSA may partly mediate the effects of OSA on  
90 adverse health outcomes, including the development of hypertension<sup>15–17</sup>. Smaller studies in  
91 humans have linked OSA to the microbiota composition in the upper airways (n = 92)<sup>18</sup> and in

92 the gut (n = 113)<sup>19</sup>. However, these studies did not adjust for important confounders, such as diet  
93 and medications, and were limited in their taxonomic resolution of the microbiota.

94 To overcome the above limitations, there is a need for adequately powered investigations  
95 of the associations between OSA and the human gut microbiota, combining extensive  
96 information on confounding factors with species-level microbiota data. Here, we used a validated  
97 method suitable for population-wide screening for OSA (ApneaLink Air®, ResMed, CA,  
98 USA)<sup>20,21</sup> to investigate how key prognostic and severity features of OSA were cross-sectionally  
99 associated with the human gut microbiota, analyzed with shotgun metagenomic sequencing in up  
100 to 3,570 participants from the large population-based Swedish CardioPulmonary BioImage  
101 Study (SCAPIS). We found that all three OSA parameters were associated with lower gut  
102 microbiota richness and evenness, as measured with the Shannon index. In addition, T90 was  
103 independently associated with 59 specific bacterial species and ODI was independently  
104 associated with 97 species. We further found that the T90-associated microbiota were enriched  
105 for nine microbial metabolic pathways. One of the T90-associated species, *Collinsella*  
106 *aerofaciens*, was also associated with systolic blood pressure independent of BMI, the OSA  
107 parameters, and related risk factors. These findings may guide future research on the role of the  
108 gut microbiota as a potential mediator of OSA-associated morbidities.

## 109 **Results**

### 110 **Descriptive statistics**

111 After excluding the participants who reported use of continuous positive air pressure (CPAP) as  
112 treatment for OSA (n = 59), the study sample consisted of 3,175 (54% female) SCAPIS  
113 participants with valid AHI data (Fig. S1) and 3,570 (52% female) with valid T90 and ODI data.  
114 The mean age was 57.7 years. The Spearman's correlation coefficient between the OSA

115 parameters was 0.56 for AHI and T90; 0.92 for AHI and ODI; and 0.63 for T90 and ODI.

116 Population characteristics are described in Table 1, as well as in Tables S1 and S2.

117

### 118 **OSA is associated with lower gut microbiota richness and evenness**

119 To investigate whether OSA was associated with the richness and evenness of the gut

120 microbiota, we performed partial Spearman's correlation analyses of the three OSA parameters

121 a) AHI, b) T90, and c) ODI with alpha diversity measured as the Shannon index<sup>22</sup>. We used a

122 hypothetical causal diagram (Fig. S2) and the d-separation criterion<sup>23</sup> to identify the minimal set

123 of confounders for adjustment in our main model. Thus, covariates in the main model consisted

124 of age, sex, smoking, alcohol intake, and BMI, as well as the DNA extraction plate to account for

125 variation between batches. We found that AHI, T90, and ODI were inversely associated with the

126 Shannon index (AHI:  $\rho = -0.058$ , p-value = 0.002; T90:  $\rho = -0.043$ , p-value = 0.013, ODI:  $\rho = -$

127  $0.065$ , p-value =  $1.75 \times 10^{-4}$ , Table S3). To better account for the influence of diet and other

128 confounders, we also constructed an extended model with additional adjustments for calculated

129 fiber intake and total energy intake from a food frequency questionnaire, self-reported leisure

130 time physical activity, education level, country of birth, and season of assessment. In this

131 extended model, the associations were somewhat attenuated (AHI:  $\rho = -0.047$ , p-value = 0.013;

132 T90:  $\rho = -0.038$ , p-value = 0.034, ODI:  $\rho = -0.055$ , p-value = 0.002). Taken together, these

133 results indicate a decreased gut microbiota richness and evenness in OSA.

134

### 135 **Gut microbiota composition differs by OSA severity independently of BMI**

136 To determine whether the OSA severity was associated with the overall gut microbiota

137 composition, we analyzed the beta diversity measured as Bray-Curtis dissimilarity in relation to

138 groups of AHI, T90, and ODI. Starting with AHI, we grouped the participants (n=3,175) with  
139 valid AHI data according to previously established and clinically used cut-off values<sup>24</sup> (no OSA:  
140 AHI < 5, n = 1,851; mild: AHI 5–14.9, n = 899; moderate: AHI 15–29.9, n = 295; severe: AHI ≥  
141 30, n = 130). To graphically represent the relationship between the groups, we conducted a  
142 principal coordinate analysis on the Bray-Curtis dissimilarity matrix (Fig. 1a). We observed a  
143 separation of the groups along the first axis in order of severity. This separation was supported  
144 by the results of a permutational analysis of variance (PERMANOVA) adjusted for the main  
145 model covariates ( $R^2 = 0.5\%$  and p-value = 0.0001). In pairwise comparisons (Table S4), we  
146 found some evidence supporting a difference for all pairwise comparisons (nominal p-value <  
147 0.05), except between the groups mild and severe (p-value = 0.26), probably due to higher  
148 dispersion and lower power in this comparison. Taken together, these results suggest that the  
149 groups of OSA severity based on AHI have different gut microbiota compositions.

150 To assess whether the gut microbiota composition also differed among participants  
151 depending on their hypoxia parameters, we divided the participants with available T90 and ODI  
152 data (n=3,570) into four groups. Because there were no well-established cut-offs, we aim to  
153 create groups of similar sizes. Due to the high proportion of participants with T90 = 0, grouping  
154 by quartiles was not possible for this variable. Therefore, we performed the following division  
155 for T90: one group of participants with T90 = 0 (n=1,088), and the remaining participants  
156 divided into three groups of similar size in order of ascending T90 values: t1 = 912 individuals  
157 (T90: 1–3%), t2 = 759 (T90: 4–14%), and t3 = 811 (T90: 15–100%). For ODI, we divided the  
158 participants by quartiles: q1 = 913 individuals (ODI: 0–1.8), q2 = 885 (ODI: 1.9–4.3), q3 = 891  
159 (ODI: 4.4–9.4), and q4 = 881 (ODI: 9.5–93). Either based on T90 or ODI, the groups separated  
160 along the first axis in order of severity in the principal coordinate analysis (Fig. 1b and 1c). We

161 confirmed the separations using PERMANOVA (T90 groups:  $R^2 = 0.2\%$  and  $p\text{-value} = 0.013$ .  
162 ODI groups:  $R^2 = 0.3\%$  and a  $p\text{-value} = 0.002$ ). In the pairwise comparisons of T90 groups  
163 (Table S4), we found that the group with T90 = 0 differed from the t2 and t3 groups ( $p\text{-values} =$   
164  $0.001$  and  $0.006$ , respectively). In the pairwise comparisons of ODI groups (Table S4), we found  
165 that the q1 group differed from the q3 and q4 groups ( $p\text{-values} = 0.014$  and  $0.001$ , respectively).  
166 We also found a difference between the q2 and q4 groups ( $p\text{-value} = 0.005$ ).

167 We additionally investigated differences in the overall gut microbiota between the groups  
168 after adjusting for the extended model covariates. For all grouping strategies; i.e., AHI-, T90- or  
169 ODI-based, we confirmed the differences in gut microbiota composition across groups (AHI  
170 groups:  $R^2 = 0.5\%$ ,  $p\text{-value} = 0.0001$ ; T90 groups:  $R^2 = 0.2\%$ ,  $p\text{-value} = 0.028$ ; ODI groups:  $R^2 =$   
171  $0.2\%$ ,  $p\text{-value} = 0.007$ ).

172 Altogether, these results point to progressive differences in the overall gut microbiota  
173 composition – as assessed with Bray-Curtis dissimilarity – across groups of OSA ordered by  
174 severity. The difference between groups was clearer when using the pre-established AHI cut-offs  
175 rather than the similarly sized groups based on T90 and ODI. We could still detect differences in  
176 the gut microbiota composition between groups of T90 or ODI even after accounting for several  
177 confounders.

178

179 **OSA-related hypoxia is associated with the relative abundance of specific gut microbiota**  
180 **species independently of BMI, dietary fiber intake, and common medications**

181 To study how the OSA parameters AHI, T90, and ODI were associated with the relative  
182 abundance of gut microbiota species, we performed a series of partial Spearman's correlations  
183 with each OSA parameter and each species. Given that BMI may influence or be influenced by



184 the abundance of gut microbiota species<sup>25</sup> and that obesity is an important cause of OSA<sup>3</sup>, BMI  
185 could either be considered a confounder or a source of reverse causation in the association of  
186 OSA with microbiota. Therefore, we divided the main model into two: one model not including,  
187 and one model including BMI. The model not including BMI was then used as a screening step  
188 to select the species that would be taken into the subsequent models. We defined significance  
189 using p-values adjusted for multiple comparisons, referred to here as q-values, with a false  
190 discovery rate set at 5%.

191 Without adjustment for BMI, we found that AHI was associated with the relative  
192 abundances of 566 species, T90 with 631 species, and ODI with 692 species (Fig. 2a and Table  
193 S5). Next, the species that were associated with at least one of the OSA parameters in this step  
194 were analyzed with the main model including BMI. In these analyses, AHI was associated with  
195 101 species, T90 with 141, and ODI with 241 (Table S6). When assessing the overlap of these  
196 associations, we found that the three OSA parameters were jointly associated with the relative  
197 abundances of 53 species. The AHI and ODI parameters were jointly associated with another 42  
198 species, ODI and T90 were jointly associated with another 46 species, and AHI and T90 were  
199 jointly associated with one other species (Fig. 2b).

200 To account for other potential confounders, the species associated with at least one of the  
201 OSA parameters in the main model not including BMI were then analyzed with the extended  
202 model. In these analyses, AHI was no longer associated with any species (Fig. 2c and Table S7).  
203 Nevertheless, T90 was associated with 59 species, of which 17 were positive, and ODI with 97  
204 species, of which 17 were positive. The parameters T90 and ODI were jointly positively  
205 associated with six species, including the species *Blautia obeum* (internal identifier:  
206 HG3A.0001), *Ruminococcus gnavus*, *Coprococcus comes*, and the recently isolated

207 *Mediterraneibacter glycyrrhizinilyticus*<sup>26</sup>. The T90 and ODI parameters were jointly negatively  
208 associated with 22 unidentified species, of which 16 belonged to the order *Eubacteriales*. Based  
209 on the correlation coefficients, the strongest positive associations with ODI were  
210 *Fusicatenibacter saccharivorans* ( $\rho = 0.069$ , q-value = 0.008), and an unidentified species of the  
211 family *Lachnospiraceae* (HG3A.0018,  $\rho = 0.069$ , q-value = 0.008). Among the 17 positive  
212 associations with ODI, 10 species belonged to the family *Lachnospiraceae*. The strongest  
213 negative association of ODI was with an unidentified *Eubacteriales* sp. (HG3A.0069,  $\rho = -0.074$ ,  
214 q-value = 0.006). The strongest positive association of T90 was with *Dorea formicigenerans* ( $\rho$   
215 = 0.086, q-value = 0.001), followed by *B. obeum* (HG3A.0001,  $\rho = 0.079$ , q-value = 0.003). The  
216 strongest negative association was with *Eubacteriales* sp. (HG3A.0703,  $\rho = -0.073$ , q-value =  
217 0.009).

218 One possible explanation for the null findings for AHI was that fewer participants had  
219 valid AHI data compared with the number of participants with valid T90 and ODI data. To  
220 ascertain that the null findings were not due to lower power, we conducted a secondary analysis  
221 where we used multiple imputations to impute missing AHI values for the 340 participants who  
222 had valid T90 or ODI values, but not valid AHI values. Even in this secondary analysis, we did  
223 not observe any associations between AHI and species after adjustment for the extended model  
224 covariates (Table S8).

225 Next, we performed a series of sensitivity analyses with the 128 species associated with  
226 T90 and/or ODI in the extended model to investigate how medication use or presence of lung  
227 disease affected our findings (Table S9). Firstly, we added to the extended model the covariates  
228 of metformin use, and proton pump inhibitor (PPI) use, based on measurable metabolomic  
229 plasma levels of these medications, as well as self-reported medication use for hypertension

230 and/or hyperlipidemia. All 128 species remained associated with T90 and/or ODI after the  
231 additional adjustment (q-value < 0.05). After excluding the 367 participants who had used any  
232 antibiotic during the six months before sampling, all associations were retained, except for the  
233 association between ODI and *Eubacteriales* sp. (HG3A.0691). The result also did not change  
234 after excluding the 29 participants with self-reported diagnosis of chronic obstructive pulmonary  
235 disease (COPD), chronic bronchitis, or pulmonary emphysema. Altogether, this series of  
236 analyses highlighted the robustness of the associations between the hypoxia parameters T90 and  
237 ODI and the identified species. In summary, we found that the OSA-related hypoxia parameters  
238 were robustly associated with 127 gut microbiota species.

239

#### 240 **The T90 and ODI associations with gut microbiota species were not modified by**

#### 241 **hemoglobin levels**

242 Exposure to hypoxia increases erythropoiesis and results in increased hemoglobin levels<sup>27</sup>. In  
243 turn, hemoglobin level affects the oxygen delivery to tissues<sup>28</sup>. To assess the effect modification  
244 by hemoglobin levels on the T90 and ODI associations with the gut microbiota species, we  
245 conducted Spearman's correlation analyses adjusted for the extended model covariates stratified  
246 by the sex-specific median hemoglobin value. These analyses included the 128 species that we  
247 identified as being associated with the T90 and/or ODI parameters (Table S10). In the  
248 association between ODI and *Eubacteriales* sp. (HG3A.1026), we detected a difference in the  
249 correlation estimates between participants with high or low hemoglobin status ( $\rho_{\text{low}} = 0.008$ , p-  
250 value<sub>low</sub> = 0.75 and  $\rho_{\text{high}} = -0.12$ , p-value<sub>high</sub> =  $1.8 \times 10^{-6}$ , heterogeneity q-value = 0.02).

251 Differences were also observed for other species, as in the association between ODI and

252 *Clostridia* sp. (HG3A.0140,  $\rho_{\text{low}} = -0.12$ , p-value<sub>low</sub> =  $4.0 \times 10^{-6}$  and  $\rho_{\text{high}} = -0.02$ , p-value<sub>high</sub> =

253 0.36), but when we formally tested for these differences, we could not confirm them  
254 (heterogeneity q-value > 0.05). Therefore, we could not ascertain whether hemoglobin levels  
255 acted as an effect modifier on the associations between OSA-related hypoxia parameters and the  
256 gut microbiota species abundance.

257

### 258 **T90-associated gut microbiota showed enriched putative metabolic pathways**

259 To characterize the putative metabolic profile of the species associated with OSA, we performed  
260 enrichment analyses to identify overrepresented metabolic pathways among the AHI, T90, or  
261 ODI associations with gut microbiota species (extended model). Metabolic pathways were  
262 defined using the gut metabolic modules (GMM)<sup>29</sup>. We found no metabolic pathways enriched in  
263 the AHI or ODI associations (Table S9). The positive associations between T90 and the gut  
264 microbiota species were enriched for nine metabolic pathways (Fig. 3a), including threonine  
265 degradation I and II (q-value =  $9.3 \times 10^{-4}$  and 0.02, respectively), and propionate production II (q-  
266 value = 0.02). The latter is comprised of the enzyme propionate CoA-transferase, which  
267 produces propionate from lactate<sup>30</sup>. The pathway threonine degradation I consists of a series of  
268 enzymatic steps that metabolize L-threonine into propionate. One of these steps is carried out  
269 by the activated pyruvate-formate lyase, which is only activated under anaerobic conditions<sup>31</sup>.  
270 The T90-species associations were also enriched for lysine degradation II (q-value = 0.004),  
271 serine degradation (q-value = 0.009), and the pathways of carbohydrate degradation:  
272 galacturonate degradation I (q-value < 0.001, and ribose degradation (q-value = 0.047).

273 Our results on the enrichment of microbial metabolic pathways suggest that the duration  
274 of hypoxia during sleep, as reflected by the T90 parameter, may favor gut microbiota species  
275 with specific metabolic repertoires. Noteworthy, we found that T90 was associated with the

276 production of propionate from lactate, a biomarker of hypoxia. On the other hand, we could not  
277 find evidence that AHI or ODI were associated with metabolic features of the gut microbiota.

278

279 **Species positively associated with T90 and/or ODI have different metabolomic fingerprints**  
280 **than those negatively associated**

281 To characterize the metabolomic fingerprint of the 128 gut microbiota species associated with  
282 T90 and/or ODI in the extended model, we mined data from the online GUTSY Atlas  
283 (<https://gutsyatlas.serve.scilifelab.se/>), which has investigated the associations between the  
284 human gut microbiota and the plasma metabolome in a cohort that also included participants  
285 from the current study<sup>32</sup>. From the GUTSY Atlas, we retrieved data on the enrichment analyses  
286 for metabolite groups in the associations between the species and the plasma metabolites. The  
287 analyses were conducted stratified by the direction of the associations.

288 In the heatmaps of enriched metabolite groups for every species, we observed a different  
289 pattern of enrichment for the 100 species that had a negative association with T90 and/or ODI  
290 values compared with the 28 species that had a positive association with these parameters. For  
291 instance, while several positively-associated species were positively associated with secondary  
292 bile acids (Fig. 4b), the negatively-associated species were negatively associated with these  
293 metabolites (Fig. 4a). A similar pattern was also observed for dihydrosphingomyelins and  
294 phosphatidylcholine metabolites. In addition, for 19 species that were negatively associated with  
295 T90/ODI, we found enrichment for vitamin A metabolites; whereas four species in positive  
296 association with T90/ODI had a negative association with vitamin A metabolites.

297 Lastly, we found evidence that the species that were negatively associated with the  
298 hypoxia parameters T90 or ODI were also negatively associated with tobacco metabolites.

299 Although these species were identified in analyses adjusted for smoking status, it is possible that  
300 these species may also have a reduced abundance in smokers, hence the negative association  
301 with tobacco metabolites.

302 Overall, our results indicated that the associations between the species and the plasma  
303 metabolites had opposite directions depending if the species abundance was expected to increase  
304 or decrease with hypoxia. The main differences in the metabolomic fingerprints involved the  
305 pattern of association with vitamin A metabolites, dihydrosphingomyelins, secondary bile acids,  
306 phosphatidylcholine, and tobacco metabolites.

307

### 308 **Microbiota species associated with OSA-related hypoxia and were also associated with** 309 **blood pressure**

310 Previous studies have found that OSA is associated with increased risk for insulin resistance<sup>33</sup>  
311 and incident blood hypertension<sup>4</sup>. Furthermore, fecal microbiota transplantation studies in mice  
312 have suggested that alterations in the gut microbiota induced by OSA might contribute to the  
313 detrimental health effects of OSA<sup>15,16</sup>. Therefore, we investigated whether the 128 T90/ODI-  
314 associated species and the nine T90-enriched metabolic pathways were also associated with  
315 blood pressure measurements (n = 2,335) and glycated hemoglobin (Hb1Ac, n = 2,786). We  
316 excluded from the association analyses with blood pressure measurements the participants who  
317 self-reported medication for hypertension. Likewise, we excluded from the analyses with HbA1c  
318 the participants who self-reported medication for diabetes. Based on a directed acyclic graph  
319 (Fig. S3), the associations were adjusted for age, sex, alcohol intake, smoking, fiber intake, total  
320 energy intake, leisure time physical activity, country of birth, ODI, AHI, T90, and DNA  
321 extraction plate. Among the species negatively associated with T90 or ODI, 19 were negatively

322 associated with systolic blood pressure (Fig. 3b), including *Intestinimonas massiliensis* ( $\rho = -$   
323 0.07, q-value = 0.02), and nine were negatively associated with diastolic blood pressure (Table  
324 S12). Among the positive associations, the species *Collinsella aerofaciens*, and the microbial  
325 pathway threonine degradation I were positively associated with systolic and diastolic blood  
326 pressure. None of the species or microbiota functions investigated were associated with Hb1Ac.

327 In the analyses additionally adjusted for BMI, *C. aerofaciens* continued to associate with  
328 systolic blood pressure ( $\rho = 0.073$ , q-value = 0.034) and *Eubacteriales* sp. (HG3A.0196)  
329 continued to negatively associate with systolic ( $\rho = -0.077$ , q-value = 0.032) and diastolic blood  
330 pressure ( $\rho = -0.081$ , q-value = 0.015). Altogether, we could observe that specific species and  
331 metabolic pathways previously identified in association with T90 or ODI were also associated  
332 with blood pressure measurements in the same direction. Two species continued to be associated  
333 with blood pressure measurements even after adjustment for BMI.

## 334 Discussion

335 Here we presented the most comprehensive population-based study to date investigating the  
336 relationship of OSA with the human gut microbiota. We found evidence that OSA, especially  
337 OSA-related hypoxia, was associated with the composition and functional potential of the human  
338 gut microbiota. The OSA hypoxia parameters, namely T90 and ODI, were associated with the  
339 abundance of specific species after extensive adjustment for potential confounders such as  
340 treatment for diabetes, hypertension, hyperlipidemia, and gastritis and gastroesophageal reflux.  
341 We further noted enrichment for specific microbial metabolic pathways shared by bacteria  
342 positively associated with the duration of hypoxia during sleep.

343 Out of the 128 species associated with T90 and/or ODI, 28 were associated with both  
344 parameters. Among the six positive associations, four were annotated to the species level,

345 namely *B. obeum*, *C. comes*, *R. gnavus*, and *M. glycyrrhizinilyticus*. A higher relative abundance  
346 of *B. obeum*, previously named *Ruminococcus obeum*, has been observed in individuals with  
347 insulin resistance<sup>34</sup>. Nevertheless, we did not find an association between *B. obeum* and HbA1c  
348 levels, a marker of glycemic control, in the present study. *C. comes* is one of the gut microbiota  
349 species found to decrease in abundance post bariatric surgery<sup>35</sup>, a procedure known to improve  
350 many conditions related to obesity, including OSA<sup>36</sup>. *R. gnavus*, a mucin-degrading microbe, has  
351 been positively associated with incident type 2 diabetes in a large Finnish population cohort<sup>37</sup>.  
352 These four species all belong to the family *Lachnospiraceae*. An increased abundance of the  
353 *Lachnospiraceae* family has been observed in mice subjected to intermittent hypoxia<sup>12</sup>. Also  
354 belonging to the same family are *D. formicigenerans* and *Anaerobutyricum hallii*, which were  
355 positively associated with T90; and *Roseburia inulinivorans*, *F. saccharivorans*, *Ruminococcus*  
356 *torques* and *Blautia massiliensis*, which were positively associated with ODI. However, a  
357 mechanistic explanation connecting the *Lachnospiraceae* family to host hypoxia is lacking and  
358 warrants further investigation.

359 In this study, ODI was positively associated with *C. aerofaciens*, which was in turn  
360 positively associated with systolic blood pressure independent of BMI and OSA. *C. aerofaciens*  
361 is an obligate anaerobe abundant in the human gut<sup>38</sup>, with higher abundance in overweight and  
362 obese individuals<sup>39</sup>. Higher abundance of *C. aerofaciens* has also been observed in individuals  
363 with type 1 pulmonary hypertension<sup>40</sup>, a condition associated with lower oxygen saturation<sup>41</sup>.  
364 Longitudinal and experimental studies are necessary to understand whether the gut microbiota  
365 species identified in this study may have a role connecting OSA to blood pressure.

366 The OSA hypoxia parameters T90 and ODI were associated with the abundance of  
367 specific species after adjustment for the extended model covariates, while AHI was not. Our



368 results suggest that OSA-related hypoxia might be of greater importance when it comes to  
369 associations with the gut microbiota than the apnea and hypopnea events themselves. Increasing  
370 attention has been given to OSA-related hypoxia, as recent studies have shown that OSA-related  
371 hypoxia, unlike AHI, predicted increased cardiovascular mortality<sup>5</sup>.

372 Evidence in the literature suggests that intermittent host hypoxia directly affects the gut  
373 microbiota. In the study by Moreno-Indias et al., intermittent hypoxia applied during the mice's  
374 rest phase resulted in enrichment for gut obligate anaerobes<sup>12</sup>. Similarly, a reduction of  
375 anaerobes was observed in the gut microbiota of rats after hyperbaric treatment<sup>42</sup>. In the Moreno-  
376 Indias et al. study, the authors demonstrated that intermittent hypoxia produced oscillations in  
377 the oxygen concentration inside the intestinal lumen close to the epithelium, thus providing a  
378 physiological rationale for how the oxygenation level of the host could impact the gut microbiota  
379 environment<sup>12</sup>.

380 The identified associations could be due to effects of OSA on sleep fragmentation as both  
381 acute and chronic sleep fragmentation have been demonstrated to affect the gut microbiota  
382 composition in rodents<sup>43</sup>. Nevertheless, sleep fragmentation alone is unlikely to explain why  
383 OSA hypoxia parameters associated with the abundance of specific species while AHI did not.  
384 Daytime sleepiness may be a result of sleep fragmentation; however, the Epworth sleepiness  
385 scale score, a measurement of daytime sleepiness, was not different between the groups of OSA  
386 severity based on T90 (Table S1). To better disentangle the effects of sleep fragmentation due to  
387 OSA from the effects of nocturnal hypoxia, future studies would benefit from concomitant  
388 electroencephalogram monitoring, polysomnography assessment and actigraphy.

389 One possible indirect mechanism through which OSA might affect the microbiota is  
390 through alterations in the host metabolism, such as accumulation of lactate<sup>44</sup>. Experiments in

391 mice using labeled lactate showed that circulating lactate can cross the gut barrier and enter the  
392 intestinal lumen<sup>45</sup>. Higher plasma concentration of lactic acid has been described in OSA  
393 patients<sup>46</sup>. Additionally, T90 was positively associated with venous concentration of lactate in  
394 treatment-naïve OSA patients<sup>44</sup>. High circulating levels of lactate is also present in athletes  
395 postexercise; although, in this case, lactate is produced in the absence of hypoxia<sup>47</sup>. A study  
396 comparing the gut microbiota in athletes before and after exercise found an increase in microbial  
397 genes involved in the conversion of lactate into propionate after exercise<sup>45</sup>. The authors of the  
398 latter study hypothesized that the host lactate entering the intestinal lumen could favor bacterial  
399 species that use lactate as a carbon source. This hypothesis corresponds with our findings; the  
400 pathway of propionate production from lactate was enriched in positive T90 associations with  
401 gut microbiota species. In summary, supported by the existing literature, our study suggests an  
402 association between the hypoxia caused by OSA, plasma lactate, and the gut microbiota  
403 metabolic profile.

404         The strengths of our study include the large sample size, temporal proximity between  
405 OSA assessment and fecal microbiota sampling, the extensive adjustment for confounders, and  
406 the use of an objective assessment for OSA instead of self-reported diagnosis or a convenience  
407 sample of OSA patients. Our investigation on a random sample from the population provides a  
408 more generalizable picture of the association between OSA and the gut microbiota than studies  
409 comparing controls to patients with a clinical diagnosis of OSA. The combination of a large  
410 sample size with shotgun metagenomic sequencing allowed us to conduct a comprehensive  
411 investigation at the species level and also of the microbial metabolic profile.

412         Nevertheless, there are limitations that need to be considered when interpreting our  
413 results. Because of the cross-sectional design, we were not able to assess causality. Despite the

414 extensive adjustment, we cannot rule out residual confounding. Moreover, even if the animal  
415 studies indicate a causal effect of OSA on the gut microbiota, an effect in opposite direction is  
416 also plausible. For example, certain gut microbiota species may promote weight gain that may  
417 consequently lead to OSA<sup>48</sup>. In this case, BMI would open a pathway for reverse causation from  
418 the gut microbiota to the development of OSA. The gut microbiota was examined using fecal  
419 shotgun metagenomics followed by detection of species based on the co-abundance of genes.  
420 Although valid and well-described<sup>49</sup>, this approach leads to the detection of some incompletely  
421 annotated species, which have not yet been isolated and characterized. Alternatively to fecal  
422 samples, mucosal biopsies could have provided information on the gut microbiota that resides  
423 more closely to the host<sup>50</sup>, thus more likely to be affected by OSA. Our results may not extend to  
424 populations in other countries due to the close connection between geographical location and the  
425 gut microbiota<sup>51</sup>. The ApneaLink Air® two-channel device used to assess sleep apnea does not  
426 distinguish obstructive from central apneas. However, obstructive sleep apneas are more  
427 common in the general population<sup>52</sup>. An assessment for OSA based on a single night may result  
428 in a certain degree of exposure misclassification<sup>53</sup>, which could affect the precision, but would  
429 not bias our estimates. The T90 parameter is not able to differentiate hypoxia caused by OSA  
430 from nocturnal hypoxia of other etiologies. Finally, we excluded participants that used CPAP, a  
431 common treatment for OSA. Thus, future studies should investigate whether the herein observed  
432 OSA-gut microbiota associations are affected by OSA therapy, including but not limited to  
433 CPAP.

434 Animal studies have found that comorbidities present in mouse models of OSA can be  
435 transferred to control mice through fecal microbial transplant<sup>15,17</sup>. Furthermore, observational  
436 studies have implicated the human gut microbiota in the development of metabolic and

437 cardiovascular disorders, such as hypertension<sup>54</sup> and insulin resistance<sup>55</sup>. Given the results from  
438 animal and observational studies, it is possible that alterations in the human gut microbiota  
439 caused by OSA could at least in part contribute to the increased risk of cardiovascular disease  
440 seen in OSA patients. Therefore, the associations that we found between OSA and the gut  
441 microbiota can be informative for future research aiming to identify gut microbiota mechanisms  
442 that connect OSA to health outcomes.

443 In conclusion, we present the largest study to date that has investigated the association  
444 between OSA and the human gut microbiota. We found that the objective parameters of OSA-  
445 related hypoxia, namely T90 and ODI, were independently associated with 59 and 97 gut  
446 microbiota species, respectively. In addition, we found that the gut microbiota associated with  
447 T90 was enriched for nine metabolic pathways, including the pathway for production of  
448 propionate from lactate. Our findings provide novel insights into the relationship between OSA  
449 and the gut microbiota. Future experimental studies are necessary to validate whether the  
450 identified microbial species may represent potential therapeutic targets to prevent or treat  
451 comorbidities of OSA.

## 452 **Methods**

### 453 **Study population**

454 From 2013 to 2018, a total of 30,154 women and men aged 50–64 were enrolled in the SCAPIS  
455 study. Participants were randomly invited from the general population across six regions in  
456 Sweden<sup>56</sup>. In the Uppsala region, 4,839 participants had data on fecal shotgun metagenomics and  
457 4,183 were assessed for OSA. Combined, 4,045 participants had both OSA data and  
458 metagenomic data. We excluded the 59 participants who reported use of CPAP. At least four  
459 hours of air flow and oxygen saturation recordings were required to compute a valid AHI value

460 and at least four hours of oxygen saturation recording was required to compute valid T90 and  
461 ODI values. Therefore, data on AHI were available for 3,175 participants and data on T90 and  
462 ODI were available for 3,570 participants (Fig. S1).

463 SCAPIS study and the present study were approved by the Swedish Ethical Review  
464 Authority (DNR 2018-315 B and amendment 2020-06597, and DNR 2010-228-31M,  
465 respectively). All participants provided informed consent.

466

#### 467 **OSA assessment**

468 Assessment for OSA was conducted using the ApneaLink Air® (ResMed, CA, USA)<sup>57</sup>. After  
469 instructions, participants took the ApneaLink Air® device home for recording of nasal air flow  
470 and oxygen saturation during one night's sleep. Apnea was defined as a reduction of breathing  
471 flow  $\geq 80\%$  for at least 10 seconds. Hypopnea was defined as a period of at least 10 seconds with  
472 a decrease in the baseline air flow of 30–80% combined with a decrease  $\geq 4\%$  in oxygen  
473 saturation. From the OSA assessment, the variables AHI, T90, and ODI were chosen for the  
474 current study as they are clinically relevant measures and commonly used in previous research.  
475 The AHI was calculated as the mean number of apneas and hypopneas events per hour of total  
476 recording time. Using clinically used cuff-off values, AHI severity groups were defined as no  
477 OSA for AHI  $< 5$ , mild for AHI 5–14.9, moderate for AHI 15–29.9, and severe for AHI  $\geq 30$ <sup>24</sup>.  
478 The T90 variable was computed by adding the time spent with an oxygen saturation  $< 90\%$  and  
479 dividing by the total recording time. For the grouping based on T90, the first group was  
480 composed of participants with a T90 = 0. The remaining participants were grouped by tertiles. It  
481 was not possible to group the participants based on quartiles because  $> 25\%$  of the participants  
482 had a T90 = 0. ODI was calculated as the mean number of desaturation events per hour during

483 the total recording time. A desaturation event was defined as a decrease from baseline  $\geq 4\%$  in  
484 oxygen saturation. For the grouping based on ODI, the participants were divided by quartiles of  
485 ODI.

486

### 487 **Fecal metagenomic analysis**

488 SCAPIS participants were instructed to collect fecal samples into dry tubes at home with the  
489 provided kit and store the samples at the home freezer until the study site visit. Median interval  
490 between fecal sample collection and OSA assessment was 0 days (IQR: 0–1). The samples were  
491 then kept at  $-20^{\circ}\text{C}$  at the test centers. After 0–7 days, the samples were shipped to the central  
492 biobank where they were kept at  $-80^{\circ}\text{C}$ . Next, the samples were sent in dry ice to Clinical  
493 Microbiomics A/S (Copenhagen, Denmark) for DNA extraction, shotgun metagenomic  
494 sequencing, and taxonomic annotation. Analyses were performed in random order of samples'  
495 boxes (16 samples per box) during 2019 and 2020. DNA was extracted from all samples using  
496 NucleoSpin® 96 Soil kits (740787; Macherey-Nagel; Germany) from the same batch (Lot:  
497 1903/001). Each extraction round contained a negative and positive control (ZymoBIOMICS™  
498 Microbial Community Standard, D6300, Zymo Research). For cell lysis, a bead beating step was  
499 performed for 5 min at 2200 rpm with tubes placed horizontally on the vortex (Vortex-Genie 2).

500 After DNA fragmentation and library preparation, sequencing was performed using an  
501 Illumina Novaseq 6000 system (Illumina, USA). On average, 26.3 million read pairs (SD =  $\pm 6.9$   
502 millions) were generated per sample for Uppsala samples. Reads were removed if they contained  
503 clear adapter contamination,  $> 10\%$  ambiguous bases, or  $> 50\%$  bases with Phred quality score  $<$   
504 5. Reads pairs were also removed if any of the reads mapped to the human reference genome  
505 GRCh38 using Bowtie 2 (v.02.3.2.)<sup>58</sup>. Reads that passed this quality control were assembled with

506 MEGAHIT (v. 1.1.1)<sup>59</sup> and mapped using BWA-MEM (v. 0.7.16a)<sup>60</sup> to a new gene catalog. This  
507 new gene catalog was created using samples from the SCAPIS study, which included samples  
508 from Uppsala and Malmö sites, samples from the Malmö Offspring Study (MOS)<sup>61</sup>, samples  
509 from Pasolli et al.<sup>62</sup>, and 3,486 publicly available genome assemblies from isolated microbial  
510 strains.

511 Co-abundant genes that passed quality assessment were defined as metagenomic species  
512 as described in Nielsen et al.<sup>49</sup>. Briefly, each metagenomic species has a gene set of 100 signature  
513 genes, which are genes selected for optimal and accurate abundance profiling. A metagenomic  
514 species was considered detected if read pairs mapped to at least three of the 100 signature genes  
515 of that metagenomic species. Then, the total gene counts were used to produce a table of  
516 metagenomic species counts, normalized according to read length. Metagenomic species counts  
517 were transformed into relative abundances.

518 There were 1,985 species identified with a mean of 355 species detected per Uppsala  
519 sample. Considering the Uppsala participants only, species that were present in  $\leq 1\%$  of the  
520 participants were removed, resulting in 1,602 species for subsequent analyses. All the negative  
521 controls showed no detectable DNA. DNA extraction from positive controls resulted in a  
522 positive signal. For the positive controls, the coefficient of variation estimated by the Shannon  
523 diversity index was 3.05%. For 158 pairs of biological replicates, the coefficient of variation was  
524 1.49%. Clinical Microbiomics was unaware that the replicates were submitted for analysis.

525 The taxonomic annotation of the metagenomic species was performed by mapping the  
526 catalog genes to NCBI RefSeq<sup>63</sup> database (downloaded on May 2, 2021). If  $>75\%$  of the  
527 metagenomic species genes mapped to a single microbial species, a species-level taxonomy was  
528 annotated to that metagenomic species. Different thresholds were used for taxonomic annotation

529 at genus, family, order, class, and phylum level (60, 50, 40, 30, and 25% respectively). However,  
530 a species or genus-level annotation was not assigned if > 10% of the genes mapped to another  
531 single species or genus. For functional annotation, the gene catalog was annotated to the  
532 EggNOG (v. 5.0) orthologous groups database (<http://eggnogdb.embl.de/>) using EggNOG-  
533 mapper-software (v. 2.0.1)<sup>64</sup>, which provides annotations to the Kyoto Encyclopedia of Genes  
534 and Genomes (KEGG) orthology (KO) database (<https://www.genome.jp/kegg/>). Based on KO  
535 annotations, the metabolic potential of the metagenomic species was determined in terms of  
536 GMM<sup>29</sup>. As previously described, the GMMs are 103 metabolic pathways, defined as a series of  
537 enzymatic steps represented by KO identifiers<sup>29</sup>. A metagenomic species was considered to  
538 contain a GMM if it contained at least two-thirds of the KOs of a module. For modules with  
539 three or fewer steps, all steps were required. For modules with alternative paths, only one path  
540 had to fulfil the criterion. The relative abundance of a GMM was defined as the sum of the  
541 relative abundances of all metagenomic species that encoded that module.

542

### 543 **Anthropometric, sociodemographic, health, and medication information**

544 SCAPIS participants answered an extensive questionnaire on demographic information,  
545 education, lifestyle, self-reported health, medication use, as well as a food frequency  
546 questionnaire<sup>65</sup>. Smoking was categorized as never, former, or current smoker. Education was  
547 categorized based on the highest level achieved. The possible education categories were  
548 uncompleted primary or lower secondary education, completed lower secondary education,  
549 upper secondary education, or university education. Leisure time physical activity was self-  
550 reported as one of four possible categories: mostly sedentary, moderate but regular exercise,  
551 moderate activity, regular and moderate activity, or regular exercise or training. According to



552 country of birth, participants were categorized into four groups: born in Scandinavia (Sweden,  
553 Denmark, Norway or Finland), in Europe, in Asia, or in other countries. From the food frequency  
554 questionnaires, variables were calculated to estimate alcohol intake (g/day)<sup>66</sup>, fiber intake  
555 (g/day)<sup>67</sup>, and total energy intake (kcal/day)<sup>66</sup>. Dietary information was assigned as missing for  
556 participants whose  $\ln(\text{total energy intake})$  was greater than the mean of  $\ln(\text{total energy intake}) \pm$   
557 3 standards deviations in the study sample. Anthropometric measurements were performed on  
558 site. BMI ( $\text{kg/m}^2$ ) was calculated as weight divided by the height squared. Systolic and diastolic  
559 blood pressure were assessed on site, calculated as the average of two measurements in the arm  
560 with the highest mean systolic pressure.

561 Anti-hypertensive medication and medication for hyperlipidemia were categorized as  
562 binary variable based on the questionnaire. Use of proton pump inhibitors (PPI) and use of  
563 metformin were defined as a binary variable based on the plasma metabolome. Participants with  
564 a measurable omeprazole and/or pantoprazole plasma level were classified as PPI users.  
565 Participants with a measurable metformin plasma level were classified as metformin users.  
566 Information on previous antibiotic use (Anatomical Therapeutical Chemical code J01) was  
567 provided by the SCAPIS cohort study after linkage with the Swedish Prescribed Drug Register  
568 ([https://www.socialstyrelsen.se/en/statistics-and-data/registers/national-prescribed-drug-](https://www.socialstyrelsen.se/en/statistics-and-data/registers/national-prescribed-drug-register/)  
569 [register/](https://www.socialstyrelsen.se/en/statistics-and-data/registers/national-prescribed-drug-register/)).

570

### 571 **Plasma metabolome analysis**

572 The fasting plasma samples were collected during site visit and stored at  $-80^{\circ}\text{C}$  in the central  
573 biobank until they were sent in random order to Metabolon Inc. (Durham, NC, USA) for  
574 metabolomics profiling, as previously described<sup>32,68</sup>. Briefly, after sample preparation,

575 metabolomics was conducted using four protocols: reverse phase (RP)/ultrahigh performance  
576 liquid chromatography–tandem mass spectroscopy (UPLC-MS/MS) with negative-ion mode  
577 electrospray ionization (ESI), hydrophilic interaction chromatography (HILIC)/UPLC-MS/MS,  
578 and two separate RP/UPLC-MS/MS resolutions with positive-ion mode ESI. Metabolites were  
579 annotated using Metabolon’s in-house compound library<sup>68</sup>. We used the GUTSY Atlas  
580 (<https://gutsyatlas.serve.scilifelab.se/>) to retrieve information on enrichment for metabolite  
581 groups in the gut microbiota species associations with plasma metabolites<sup>32</sup>.

582

### 583 **Statistical analyses**

584 To identify the set of confounders for adjustment, we created a hypothetical causal diagram in  
585 the browser-based application DAGitty 3.0 ([www.dagitty.net](http://www.dagitty.net); Fig. S2)<sup>69</sup>. To investigate the  
586 association between OSA and the gut microbiota, we identified sex, age, smoking, alcohol  
587 intake, and BMI as the minimal sufficient adjustment set. Therefore, these variables were  
588 included in the main model together with DNA extraction plate to account for technical  
589 variation. Age, alcohol intake, and BMI were modelled as continuous variables. Sex and  
590 smoking were modelled as categorical variables. DNA extraction plate was also modelled as a  
591 categorical variable with one level per plate (i.e., 52 levels). Given that the hypothetical causal  
592 diagram on the effect of OSA on the gut microbiota is rather complex and that confounders such  
593 as diet<sup>70</sup> and socioeconomic status<sup>71</sup> were not included in the minimal sufficient adjustment set,  
594 we chose to construct an extended model accounting for these factors. Thus, the extended model  
595 additionally included fiber intake, total energy intake, leisure time physical activity, highest  
596 education level achieved, country of birth, and season. Fiber intake and total energy intake were  
597 modelled as continuous variables. Leisure time physical activity, highest education level, and

598 country of birth were modelled as categorical variables with four levels each. The variable  
599 season consisted of 11 categories based on the month of the study site visit. The categories  
600 “June” and “July” were merged because there were only four participants for July.

601 Analyses were conducted using the R software version 4.1.1 (<https://cran.r-project.org/>).  
602 Partial Spearman’s correlations were performed using the function *pcor.test* in the R package  
603 *ppcor*<sup>72</sup>. Gut microbiota beta diversity and alpha diversity were calculated using the package  
604 *vegan* version 2.5-7<sup>73</sup>. For the alpha diversity analyses, the Shannon index<sup>22</sup> was calculated for  
605 each participant using the function *diversity*. To investigate how AHI, T90 and ODI were  
606 associated with the Shannon index, we used partial Spearman’s correlation. The beta diversity  
607 was assessed with the Bray-Curtis dissimilarity, which was calculated using the function *vegdist*.  
608 PERMANOVA was conducted using the function *adonis2* (package *vegan*) with 9,999  
609 permutations assessing the marginal effects of the terms. The Bray-Curtis dissimilarity matrix  
610 was set as the outcome and the AHI, T90, or ODI severity groups were set as the main exposure  
611 separately. Principal coordinate analysis was conducted using the function *pcoa* from the  
612 package *ape*<sup>74</sup>.

613 To investigate how AHI, T90, and ODI associated with the relative abundance of the gut  
614 microbiota species, we examined the partial Spearman’s correlation between each of the OSA  
615 parameters and each of the 1,602 species. To understand the effect of BMI on our results, we  
616 first conducted this analysis with the main model not including the covariate BMI. The species  
617 identified in this first step were further investigated in two additional analyses: one with all main  
618 model covariates, including BMI, and another model including the extended model covariates.  
619 Multiple comparison was accounted for using the Benjamini-Hochberg method with a FDR set at  
620 5%<sup>75</sup>.

621 The species associated with at least one of the three OSA parameters in the extended  
622 model were further examined in three sensitivity analyses. In the first sensitivity analysis, we  
623 included to the extended model the variables of medication use, more specifically metformin,  
624 PPI, anti-hypertensive medications, and/or medications for hyperlipidemia. In the second  
625 sensitivity analysis, we excluded participants (n = 367 among those with valid T90/ODI values)  
626 that had used any antibiotic in the previous six months. And in the third sensitivity analysis, we  
627 excluded the 29 participants with lung disease, defined as a self-reported diagnosis of COPD,  
628 chronic bronchitis, or pulmonary emphysema. After removing these participants, we re-  
629 conducted the Spearman's correlation analyses adjusting for the extended model covariates.

630 We handled missing data using complete-case analysis; i.e., participants that did not have  
631 information for all variables included in a model were removed from that respective analysis.  
632 The variable with the highest frequency of missing information was leisure time physical activity  
633 followed by smoking, antihypertensive medication use, and use of medication for  
634 hyperlipidemia. Of the participants with valid AHI data, 6% were missing information for leisure  
635 time physical activity. Information on smoking, anti-hypertensive medication, and medication  
636 for hyperlipidemia was missing for 5% of the participants who had valid AHI data. After  
637 removing participants with incomplete information on the main model covariates, there were  
638 3,004 participants for AHI analyses and 3,364 participants for the T90 and ODI analyses. Adding  
639 or removing BMI did not change the number of participants included, as this variable was not  
640 missing for all participants. For the extended model, after removing participants with incomplete  
641 information on covariates, there were 2,909 participants for the AHI analyses and 3,249  
642 participants for the T90 and ODI analyses. In the sensitivity analysis adjusting for medication  
643 use, there were 3,305 participants for the T90 and ODI analyses.

644 Because of the lower number of participants with valid AHI values than the number of  
645 participants with valid T90 and ODI values, we conducted a secondary analysis where we  
646 imputed the AHI values for the 340 participants that for whom we had information on T90 and  
647 ODI but not on AHI, considering the extended model covariates. This analysis was conducted  
648 using the software Stata 15.1 (Stata Corp., Texas, USA). Multiple imputation was conducted  
649 using predicted mean matching with the five nearest neighbors and 10 imputations. Variables  
650 used for imputation included all extended model covariates, as well as Shannon index, AHI, T90,  
651 ODI, waist-hip-ratio, and the species relative abundance. To avoid including all 1,602 species in  
652 the same imputation equation, we performed an imputation step for each species, followed by the  
653 Spearman's correlation analysis between AHI and the species, adjusted for the extended model  
654 covariates. The uncertainty of imputations was accounted for using Rubin's combination rules<sup>76</sup>.

655 The effect modification by hemoglobin level was explored by categorizing participants  
656 into low or high hemoglobin groups based on the sex-specific median hemoglobin level. First,  
657 we conducted the Spearman's correlation of OSA parameters with species relative abundance  
658 stratified by hemoglobin group and adjusted for the extended model covariates. Next, each pair  
659 of correlation coefficients obtained from the two groups were compared as described in Altman  
660 et al.<sup>77</sup> Briefly, the standard error for each coefficient was estimated using 1,000 bootstrap  
661 replications (R package *boot*<sup>78</sup>). Z-scores were then calculated as the ratio of the difference  
662 between the two coefficients to the standard error of the difference. The two-sided p-values were  
663 then obtained from the standard normal distribution.

664 For the pathway enrichment analysis for GMM, we used the Spearman's correlation  
665 results from the extended model on the associations of AHI, T90, and ODI with the 1,602  
666 microbiota species. The enrichment analyses were conducted based on ranked p-values using the

667 R package *fgsea*<sup>79</sup>, stratified by the direction of the correlation coefficients. To investigate the  
668 metabolite groups associated with each T90/ODI-associated species, we retrieved from GUTSY  
669 Atlas<sup>32</sup> the enrichment analysis results for metabolite groups for each of the species.

670 In a post hoc analysis, we used Spearman's correlation to assess the association of our  
671 main gut microbiota findings with systolic and diastolic blood pressure, as well as HbA1c. To  
672 decide on the set of covariates for adjustment, we created a hypothetical causal diagram of the  
673 effect of the gut microbiota on blood pressure and insulin resistance (Fig. S3). Based on the  
674 causal diagram, we adjusted the analysis for age, sex, alcohol intake, smoking, fiber intake, total  
675 energy intake, leisure time physical activity, country of birth, ODI, T90, and AHI, in addition to  
676 DNA extraction plates. Due to the effect of medication on the gut microbiota and the health  
677 outcomes of interest, we excluded the participants who self-reported medication use for  
678 hypertension from the analyses with blood pressure measurements. In the analyses of the  
679 association with HbA1c, we excluded participants who self-reported medication use for diabetes.  
680 Using a complete-case analysis, data were available for 2,335 participants for the analyses with  
681 blood pressure measurements and for 2,801 participants for the Hb1Ac analyses. Lastly, we  
682 assessed the effect of adding BMI to the model.

### 683 **Data availability**

684 The anonymized metagenomic sequences can be found in the European Nucleotide Archive  
685 under the accession code "PRJEB51353". The individual-level data underlying this article were  
686 provided by the SCAPIS cohort study under agreement, after ethical approval, and are not shared  
687 publicly due to confidentiality. Data will be shared upon reasonable request to the corresponding  
688 author only after permission by the SCAPIS Data access board ([https://www.scapis.org/data-](https://www.scapis.org/data-access/)  
689 [access/](https://www.scapis.org/data-access/)) and by the Swedish Ethical Review Authority (<https://etikprovningmyndigheten.se>).

690 **Code availability**

691 The code used in the present analyses is available at GitHub

692 ([https://github.com/MolEpicUU/sleepapnea\\_gut](https://github.com/MolEpicUU/sleepapnea_gut))

693 **References**

- 694 1. Jordan, A. S., McSharry, D. G. & Malhotra, A. Adult obstructive sleep apnoea. *Lancet Lond.*  
695 *Engl.* **383**, 736–747 (2014).
- 696 2. Benjafield, A. V. *et al.* Estimation of the global prevalence and burden of obstructive sleep  
697 apnoea: a literature-based analysis. *Lancet Respir. Med.* **7**, 687–698 (2019).
- 698 3. Schwartz, A. R. *et al.* Obesity and obstructive sleep apnea: pathogenic mechanisms and  
699 therapeutic approaches. *Proc. Am. Thorac. Soc.* **5**, 185–192 (2008).
- 700 4. Peppard, P. E., Young, T., Palta, M. & Skatrud, J. Prospective study of the association  
701 between sleep-disordered breathing and hypertension. *N. Engl. J. Med.* **342**, 1378–1384  
702 (2000).
- 703 5. Azarbarzin, A. *et al.* The hypoxic burden of sleep apnoea predicts cardiovascular disease-  
704 related mortality: the Osteoporotic Fractures in Men Study and the Sleep Heart Health Study.  
705 *Eur. Heart J.* **40**, 1149–1157 (2019).
- 706 6. Collen, J., Lettieri, C., Wickwire, E. & Holley, A. Obstructive sleep apnea and  
707 cardiovascular disease, a story of confounders! *Sleep Breath.* **24**, 1299–1313 (2020).
- 708 7. Linz, D. *et al.* Nocturnal hypoxemic burden is associated with epicardial fat volume in  
709 patients with acute myocardial infarction. *Sleep Breath.* **22**, 703–711 (2018).
- 710 8. Khoshkish, S. *et al.* The association between different features of sleep-disordered breathing  
711 and blood pressure: A cross-sectional study. *J. Clin. Hypertens. Greenwich Conn* **20**, 575–  
712 581 (2018).

- 713 9. Terrill, P. I. A review of approaches for analysing obstructive sleep apnoea-related patterns  
714 in pulse oximetry data. *Respirology* **25**, 475–485 (2020).
- 715 10. Rashid, N. H. *et al.* The Value of Oxygen Desaturation Index for Diagnosing Obstructive  
716 Sleep Apnea: A Systematic Review. *The Laryngoscope* **131**, 440–447 (2021).
- 717 11. Salvucci, E. The human-microbiome superorganism and its modulation to restore health. *Int.*  
718 *J. Food Sci. Nutr.* **70**, 781–795 (2019).
- 719 12. Moreno-Indias, I. *et al.* Intermittent hypoxia alters gut microbiota diversity in a mouse model  
720 of sleep apnoea. *Eur. Respir. J.* **45**, 1055–1065 (2015).
- 721 13. Lucking, E. F. *et al.* Chronic intermittent hypoxia disrupts cardiorespiratory homeostasis and  
722 gut microbiota composition in adult male guinea-pigs. *EBioMedicine* **38**, 191–205 (2018).
- 723 14. Tripathi, A. *et al.* Intermittent Hypoxia and Hypercapnia, a Hallmark of Obstructive Sleep  
724 Apnea, Alters the Gut Microbiome and Metabolome. *mSystems* **3**, e00020-18.
- 725 15. Durgan, D. J. *et al.* Role of the Gut Microbiome in Obstructive Sleep Apnea-Induced  
726 Hypertension. *Hypertens. Dallas Tex 1979* **67**, 469–474 (2016).
- 727 16. Khalyfa, A. *et al.* Circulating exosomes and gut microbiome induced insulin resistance in  
728 mice exposed to intermittent hypoxia: Effects of physical activity. *EBioMedicine* **64**, 103208  
729 (2021).
- 730 17. Badran, M., Khalyfa, A., Ericsson, A. & Gozal, D. Fecal microbiota transplantation from  
731 mice exposed to chronic intermittent hypoxia elicits sleep disturbances in naïve mice. *Exp.*  
732 *Neurol.* **334**, 113439 (2020).
- 733 18. Hong, S.-N. *et al.* Association of obstructive sleep apnea severity with the composition of the  
734 upper airway microbiome. *J. Clin. Sleep Med. JCSM Off. Publ. Am. Acad. Sleep Med.* (2021)  
735 doi:10.5664/jcsm.9640.



- 736 19. Ko, C.-Y. *et al.* Gut microbiota in obstructive sleep apnea-hypopnea syndrome: disease-  
737 related dysbiosis and metabolic comorbidities. *Clin. Sci. Lond. Engl.* 1979 **133**, 905–917  
738 (2019).
- 739 20. Ng, S. S. S. *et al.* Validation of a portable recording device (ApneaLink) for identifying  
740 patients with suspected obstructive sleep apnoea syndrome. *Intern. Med. J.* **39**, 757–762  
741 (2009).
- 742 21. Prudon, B., Hughes, J. & West, S. A novel postal-based approach to diagnosing obstructive  
743 sleep apnoea in a high-risk population. *Sleep Med.* **33**, 1–5 (2017).
- 744 22. Spellerberg, I. F. & Fedor, P. J. A tribute to Claude Shannon (1916–2001) and a plea for  
745 more rigorous use of species richness, species diversity and the ‘Shannon–Wiener’ Index.  
746 *Glob. Ecol. Biogeogr.* **12**, 177–179 (2003).
- 747 23. Pearl, J. Causal Diagrams for Empirical Research. *Biometrika* **82**, 669–688 (1995).
- 748 24. Sleep-Related Breathing Disorders in Adults: Recommendations for Syndrome Definition  
749 and Measurement Techniques in Clinical Research. *Sleep* **22**, 667–689 (1999).
- 750 25. Meijnikman, A. S., Gerdes, V. E., Nieuwdorp, M. & Herrema, H. Evaluating Causality of  
751 Gut Microbiota in Obesity and Diabetes in Humans. *Endocr. Rev.* **39**, (2018).
- 752 26. Togo, A. H. *et al.* Description of *Mediterraneibacter massiliensis*, gen. nov., sp. nov., a new  
753 genus isolated from the gut microbiota of an obese patient and reclassification of  
754 *Ruminococcus faecis*, *Ruminococcus lactaris*, *Ruminococcus torques*, *Ruminococcus gnavus*  
755 and *Clostridium glycyrrhizinilyticum* as *Mediterraneibacter faecis* comb. nov.,  
756 *Mediterraneibacter lactaris* comb. nov., *Mediterraneibacter torques* comb. nov.,  
757 *Mediterraneibacter gnavus* comb. nov. and *Mediterraneibacter glycyrrhizinilyticus* comb.  
758 nov. *Antonie Van Leeuwenhoek* **111**, 2107–2128 (2018).

- 759 27. Kaelin, W. G. & Ratcliffe, P. J. Oxygen sensing by metazoans: the central role of the HIF  
760 hydroxylase pathway. *Mol. Cell* **30**, 393–402 (2008).
- 761 28. Feiner, J. R. *et al.* High Oxygen Partial Pressure Decreases Anemia-Induced Heart Rate  
762 Increase Equivalent to Transfusion. *Anesthesiology* **115**, 492–498 (2011).
- 763 29. Vieira-Silva, S. *et al.* Species-function relationships shape ecological properties of the  
764 human gut microbiome. *Nat. Microbiol.* **1**, 16088 (2016).
- 765 30. Selmer, T., Willanzheimer, A. & Hetzel, M. Propionate CoA-transferase from *Clostridium*  
766 propionicum. *Eur. J. Biochem.* **269**, 372–380 (2002).
- 767 31. Sawers, G. & Watson, G. A glycyl radical solution: oxygen-dependent interconversion of  
768 pyruvate formate-lyase. *Mol. Microbiol.* **29**, 945–954 (1998).
- 769 32. Dekkers, K. F. *et al.* An online atlas of human plasma metabolite signatures of gut  
770 microbiome composition. Preprint at  
771 <https://www.medrxiv.org/content/10.1101/2021.12.23.21268179v1> (2021).
- 772 33. Priou, P. *et al.* Independent association between obstructive sleep apnea severity and  
773 glycated hemoglobin in adults without diabetes. *Diabetes Care* **35**, 1902–1906 (2012).
- 774 34. Zhang, X., Zhao, A., Sandhu, A. K., Edirisinghe, I. & Burton-Freeman, B. M. Functional  
775 Deficits in Gut Microbiome of Young and Middle-Aged Adults with Prediabetes Apparent in  
776 Metabolizing Bioactive (Poly)phenols. *Nutrients* **12**, E3595 (2020).
- 777 35. Graessler, J. *et al.* Metagenomic sequencing of the human gut microbiome before and after  
778 bariatric surgery in obese patients with type 2 diabetes: correlation with inflammatory and  
779 metabolic parameters. *Pharmacogenomics J.* **13**, 514–522 (2013).
- 780 36. Wong, A.-M. *et al.* The effect of surgical weight loss on obstructive sleep apnoea: A  
781 systematic review and meta-analysis. *Sleep Med. Rev.* **42**, 85–99 (2018).

- 782 37. Ruuskanen, M. O. *et al.* Gut Microbiome Composition Is Predictive of Incident Type 2  
783 Diabetes in a Population Cohort of 5,572 Finnish Adults. *Diabetes Care* **45**, 811–818 (2022).
- 784 38. Bag, S., Ghosh, T. S. & Das, B. Complete Genome Sequence of *Collinsella aerofaciens*  
785 Isolated from the Gut of a Healthy Indian Subject. *Genome Announc.* **5**, e01361-17 (2017).
- 786 39. Companys, J. *et al.* Gut Microbiota Profile and Its Association with Clinical Variables and  
787 Dietary Intake in Overweight/Obese and Lean Subjects: A Cross-Sectional Study. *Nutrients*  
788 **13**, (2021).
- 789 40. Kim, S. *et al.* Altered Gut Microbiome Profile in Patients with Pulmonary Arterial  
790 Hypertension. *Hypertens. Dallas Tex 1979* **75**, 1063–1071 (2020).
- 791 41. Galiè, N. *et al.* Guidelines for the diagnosis and treatment of pulmonary hypertension: the  
792 Task Force for the Diagnosis and Treatment of Pulmonary Hypertension of the European  
793 Society of Cardiology (ESC) and the European Respiratory Society (ERS), endorsed by the  
794 International Society of Heart and Lung Transplantation (ISHLT). *Eur. Heart J.* **30**, 2493–  
795 2537 (2009).
- 796 42. Maity, C., Adak, A., Pathak, T. K., Pati, B. R. & Chandra Mondal, K. Study of the cultivable  
797 microflora of the large intestine of the rat under varied environmental hyperbaric pressures.  
798 *J. Microbiol. Immunol. Infect.* **45**, 281–286 (2012).
- 799 43. Triplett, J., Braddock, A., Roberts, E., Ellis, D. & Chan, V. Identification of sleep  
800 fragmentation-induced gut microbiota alteration and prediction of functional impact in  
801 Sprague Dawley rats harboring microbiome derived from multiple human donors. *Sleep Sci.*  
802 *Sao Paulo Braz.* **15**, 07–19 (2022).
- 803 44. Lin, T. *et al.* The effect of CPAP treatment on venous lactate and arterial blood gas among  
804 obstructive sleep apnea syndrome patients. *Sleep Breath.* **21**, 303–309 (2017).

- 805 45. Scheiman, J. *et al.* Meta-omics analysis of elite athletes identifies a performance-enhancing  
806 microbe that functions via lactate metabolism. *Nat. Med.* **25**, 1104–1109 (2019).
- 807 46. Xu, H. *et al.* Metabolomics Profiling for Obstructive Sleep Apnea and Simple Snorers. *Sci.*  
808 *Rep.* **6**, 30958 (2016).
- 809 47. Poole, D. C., Rossiter, H. B., Brooks, G. A. & Gladden, L. B. The anaerobic threshold: 50+  
810 years of controversy. *J. Physiol.* **599**, 737–767 (2021).
- 811 48. Muscogiuri, G. *et al.* Gut microbiota: a new path to treat obesity. *Int. J. Obes. Suppl.* **9**, 10–  
812 19 (2019).
- 813 49. Nielsen, H. B. *et al.* Identification and assembly of genomes and genetic elements in  
814 complex metagenomic samples without using reference genomes. *Nat. Biotechnol.* **32**, 822–  
815 828 (2014).
- 816 50. Tap, J. *et al.* Identification of an Intestinal Microbiota Signature Associated With Severity of  
817 Irritable Bowel Syndrome. *Gastroenterology* **152**, 111-123.e8 (2017).
- 818 51. Vangay, P. *et al.* US Immigration Westernizes the Human Gut Microbiome. *Cell* **175**, 962–  
819 972.e10 (2018).
- 820 52. Donovan, L. M. & Kapur, V. K. Prevalence and Characteristics of Central Compared to  
821 Obstructive Sleep Apnea: Analyses from the Sleep Heart Health Study Cohort. *Sleep* **39**,  
822 1353–1359 (2016).
- 823 53. Lechat, B. *et al.* Multinight Prevalence, Variability, and Diagnostic Misclassification of  
824 Obstructive Sleep Apnea. *Am. J. Respir. Crit. Care Med.* **205**, 563–569 (2022).
- 825 54. Li, J. *et al.* Gut microbiota dysbiosis contributes to the development of hypertension.  
826 *Microbiome* **5**, 14 (2017).

- 827 55. Pedersen, H. K. *et al.* Human gut microbes impact host serum metabolome and insulin  
828 sensitivity. *Nature* **535**, 376–381 (2016).
- 829 56. Bergström, G. *et al.* Prevalence of Subclinical Coronary Artery Atherosclerosis in the  
830 General Population. *Circulation* **144**, 916–929 (2021).
- 831 57. Byun, J.-I., Song, S. J., Cha, H.-K. & Shin, W. C. Reliability of Manual and Automatic  
832 Scoring of Single Channel Nasal Airflow Device (ApneaLink) in Determining Moderate or  
833 Severe Obstructive Sleep Apnea Syndrome. *Sleep Med. Res.* **7**, 68–73 (2016).
- 834 58. Langmead, B. & Salzberg, S. L. Fast gapped-read alignment with Bowtie 2. *Nat. Methods* **9**,  
835 357–359 (2012).
- 836 59. Li, D., Liu, C.-M., Luo, R., Sadakane, K. & Lam, T.-W. MEGAHIT: an ultra-fast single-  
837 node solution for large and complex metagenomics assembly via succinct de Bruijn graph.  
838 *Bioinforma. Oxf. Engl.* **31**, 1674–1676 (2015).
- 839 60. Li, H. & Durbin, R. Fast and accurate short read alignment with Burrows-Wheeler transform.  
840 *Bioinforma. Oxf. Engl.* **25**, 1754–1760 (2009).
- 841 61. Brunkwall, L. *et al.* The Malmö Offspring Study (MOS): design, methods and first results.  
842 *Eur. J. Epidemiol.* **36**, 103–116 (2021).
- 843 62. Pasolli, E. *et al.* Extensive Unexplored Human Microbiome Diversity Revealed by Over  
844 150,000 Genomes from Metagenomes Spanning Age, Geography, and Lifestyle. *Cell* **176**,  
845 649–662.e20 (2019).
- 846 63. Haft, D. H. *et al.* RefSeq: an update on prokaryotic genome annotation and curation. *Nucleic*  
847 *Acids Res.* **46**, D851–D860 (2018).
- 848 64. Huerta-Cepas, J. *et al.* Fast Genome-Wide Functional Annotation through Orthology  
849 Assignment by eggNOG-Mapper. *Mol. Biol. Evol.* **34**, 2115–2122 (2017).

- 850 65. Bergström, G. *et al.* The Swedish CARDioPulmonary BioImage Study: objectives and design.  
851 *J. Intern. Med.* **278**, 645–659 (2015).
- 852 66. Christensen, S. E. *et al.* Two New Meal- and Web-Based Interactive Food Frequency  
853 Questionnaires: Validation of Energy and Macronutrient Intake. *J. Med. Internet Res.* **15**,  
854 e109 (2013).
- 855 67. Christensen, S. E. *et al.* Relative Validity of Micronutrient and Fiber Intake Assessed With  
856 Two New Interactive Meal- and Web-Based Food Frequency Questionnaires. *J. Med.*  
857 *Internet Res.* **16**, e59 (2014).
- 858 68. Evans, A. M., DeHaven, C. D., Barrett, T., Mitchell, M. & Milgram, E. Integrated,  
859 Nontargeted Ultrahigh Performance Liquid Chromatography/Electrospray Ionization  
860 Tandem Mass Spectrometry Platform for the Identification and Relative Quantification of  
861 the Small-Molecule Complement of Biological Systems. *Anal. Chem.* **81**, 6656–6667 (2009).
- 862 69. Textor, J., van der Zander, B., Gilthorpe, M. S., Liškiewicz, M. & Ellison, G. T. Robust  
863 causal inference using directed acyclic graphs: the R package ‘dagitty’. *Int. J. Epidemiol.* **45**,  
864 1887–1894 (2016).
- 865 70. Bolte, L. A. *et al.* Long-term dietary patterns are associated with pro-inflammatory and anti-  
866 inflammatory features of the gut microbiome. *Gut* **70**, 1287–1298 (2021).
- 867 71. Bowyer, R. C. E. *et al.* Socioeconomic Status and the Gut Microbiome: A TwinsUK Cohort  
868 Study. *Microorganisms* **7**, E17 (2019).
- 869 72. Kim, S. ppcor: An R Package for a Fast Calculation to Semi-partial Correlation Coefficients.  
870 *Commun. Stat. Appl. Methods* **22**, 665–674 (2015).
- 871 73. R Core Team. R: A language and environment for statistical computing. (2021).

- 872 74. Paradis, E., Claude, J. & Strimmer, K. APE: Analyses of Phylogenetics and Evolution in R  
873 language. *Bioinformatics* **20**, 289–290 (2004).
- 874 75. Benjamini, Y. & Hochberg, Y. Controlling the False Discovery Rate: A Practical and  
875 Powerful Approach to Multiple Testing. *J. R. Stat. Soc. Ser. B Methodol.* **57**, 289–300  
876 (1995).
- 877 76. Rubin, D. B. *Multiple Imputation for Nonresponse in Surveys*. (John Wiley & Sons, 2004).
- 878 77. Altman, D. G. & Bland, J. M. Interaction revisited: the difference between two estimates.  
879 *BMJ* **326**, 219 (2003).
- 880 78. Canty, A. & Ripley, B. boot: Bootstrap R (S-Plus) Functions. (2021).
- 881 79. Korotkevich, G. *et al.* Fast gene set enrichment analysis. 060012 (2021) doi:10.1101/060012.  
882

## 883 **Acknowledgements**

884 We would like to acknowledge the financial support from the European Research Council [ERC-  
885 2018-STG801965 (TF); ERC-CoG-2014-649021 (MO-M); ERC-STG-2015-679242 (JGS)], the  
886 Swedish Heart-Lung Foundation [Hjärt-Lungfonden, 2019-0505 (TF); 2020-0485 (EL); 2018-  
887 0343 (JÄ); 2020-0711 (MO-M); 2020-0173 (GE); 2019-0526 (JGS)], the Swedish Research  
888 Council [VR, 2019-01471 (TF), 2018-02784 (MO-M), 2019-01015 (JÄ), 2020-00243 (JÄ),  
889 2019-01236 (GE), 2021-02273 (JGS)], the Swedish Research Council for Sustainable  
890 Development [FORMAS, 2020-00989 (SA)], EASD/Novo Nordisk (SA), Göran Gustafsson  
891 foundation [2016 (TF)], Axel and Signe Lagerman's foundation (TF), and governmental funding  
892 of clinical research within the Swedish National Health Service (JGS).

893 We acknowledge the SCAPIS board for enabling the current study, along with the  
894 Swedish Heart-Lung Foundation, the main funding body of SCAPIS. Funding for the SCAPIS

895 study was also provided by the Knut and Alice Wallenberg Foundation, the Swedish Research  
896 Council and VINNOVA (Sweden's Innovation agency) the University of Gothenburg and  
897 Sahlgrenska University Hospital, Karolinska Institutet and Stockholm County council,  
898 Linköping University and University Hospital, Lund University and Skåne University Hospital,  
899 Umeå University and University Hospital, Uppsala University and University Hospital. The  
900 computations and data handling were enabled by resources in project sens2019512 provided by  
901 the Swedish National Infrastructure for Computing (SNIC) at Uppsala Multidisciplinary Center  
902 for Advanced Computational Science (UPPMAX), partially funded by the Swedish Research  
903 Council through grant agreement no. 2018-05973.

#### 904 **Competing interests**

905 J.B.H. and H.B.N. are currently working at Clinical Microbiomics A/S. J.Ä. has served on the  
906 advisory boards for AstraZeneca and Boehringer Ingelheim and has received lecturing fees from  
907 AstraZeneca and Novartis, all unrelated to the present work. C.B. served as a scientific  
908 consultant for Repha GmbH, Langenhagen, Germany between 2020 and 2021. JS has stock  
909 ownership in companies providing services to Amgen, AstraZeneca, Boehringer, Bayer, Eli  
910 Lilly, Itrim, Janssen, Novo Nordisk, Pfizer and Takeda, outside the submitted work. The  
911 remaining authors declare no competing interests.

#### 912 **Contributions**

913 EL, LL, JS, GB, GE, JGS, JÄ, MO-M and TF obtained the funding for the study. GBa, SS-B, JT-  
914 H, UH, BK, EL and TF planned and designed the study. JBH and HBN supervised the fecal  
915 samples processing and metagenomics bioinformatics analyses at Clinical Microbiomics S/A.  
916 GBa carried out the statistical analyses with contribution from SS-B, KD, and UH. GBa wrote



917 first version of the manuscript with support from SS-B, JT-H, BK, EL, and TF. All authors  
918 contributed with the critical interpretation of the results and critical revision of the manuscript.

## 919 **Figure captions**

920 **Figure 1.** Principal coordinate analysis showing progressive differences in the overall gut  
921 microbiota composition, measured with Bray-Curtis dissimilarity, across groups of obstructive  
922 sleep apnea (OSA) severity. Closed circles represent the mean axis value per group and bars  
923 represent the standard errors. The percentages on the axes labels represent the variance explained  
924 by each axis. **a.** AHI severity groups. No OSA: AHI < 5; Mild: AHI 5–14.9; Moderate: AHI 15–  
925 29.9; Severe: AHI  $\geq$  30. **b.** T90 severity groups were defined as one category including  
926 participants with T90 = 0, and the remaining participants divided by tertiles (t1: T90 = 1–3; t2:  
927 T90 = 4–14; and t3: T90  $\geq$  15). **c.** ODI severity groups were defined by quartiles of ODI (q1:  
928 ODI = 0–1.8; q2: ODI = 1.9–4.3; q3: ODI = 4.4–9.4; and q4: ODI  $\geq$  9.5). AHI: apnea-hypopnea  
929 index; ODI: oxygen desaturation index; PCo: principal coordinate; T90: percentage of time with  
930 oxygen saturation < 90%.

931

932 **Figure 2.** Number of microbiota species associated with AHI, T90, and/or ODI. Associations  
933 investigated using partial Spearman’s correlation after removing participants with missing data  
934 on covariates. Adjustment for multiple comparisons using the Benjamini-Hochberg method with  
935 a 5% false discovery rate. **a.** Results from the main model (i.e., adjustment for age, sex, smoking,  
936 alcohol intake, and DNA extraction plate) not including adjustment for body mass index (BMI)  
937 and **b.** including adjustment for BMI. For AHI, n = 3004. For T90 and ODI, n = 3,364. **c.** Results  
938 from the extended model (i.e., further adjustment for fiber intake, total energy intake, leisure  
939 time physical activity, education, country of birth, and season). For AHI, n = 2,909. For T90 and

940 ODI, n = 3,249. AHI: apnea-hypopnea index; ODI: oxygen desaturation index; T90: percentage  
941 of time with oxygen saturation < 90%.

942

943 **Figure 3. a.** Enrichment for gut metabolic modules (GMM) among the positive associations  
944 between T90 and gut microbiota species. The pathway enrichment analysis was conducted on the  
945 ranked p-values obtained from Spearman's correlations adjusted for age, sex, alcohol intake,  
946 smoking, body mass index, fiber intake, total energy intake, leisure time physical activity,  
947 education, country of birth, season, and DNA extraction plate. Multiple comparisons were  
948 adjusted for using the Benjamini-Hochberg method. q-values: adjusted p-values considering a  
949 5% false discovery rate **b.** Heatmap showing the species associated with T90 or ODI and the  
950 T90-enriched GMM<sup>(1)</sup> that were also associated with at least one of the health outcomes: systolic  
951 blood pressure (SBP), diastolic blood pressure (DBP), and glycated hemoglobin (Hb1Ac). OSA  
952 adj: Spearman's correlation adjusted for age, sex, alcohol intake, smoking, fiber intake, total  
953 energy intake, leisure time physical activity, country of birth, apnea-hypopnea index (AHI),  
954 oxygen desaturation index, T90, and DNA extraction plate. OSA+BMI adj: additional  
955 adjustment for body mass index (BMI). Associations with an asterisk (\*) were identified  
956 considering a 5% false discovery rate. NES: normalized enrichment score; OSA: obstructive  
957 sleep apnea; T90: percentage of time with oxygen saturation < 90%.

958

959 **Figure 4.** Relationship of the T90- and/or ODI-associated species with the plasma metabolome.  
960 T90 and ODI were **a.** negatively associated with 100 species and **b.** positively associated with 28  
961 species. The heatmaps show the enriched metabolites groups in the associations between species  
962 and metabolites stratified by the direction of the associations. Enrichment results retrieved from

963 the GUTSY Atlas (<https://gutsyatlas.serve.scilifelab.se/>)<sup>32</sup>. Multiple comparisons were adjusted  
964 for using the Benjamini-Hochberg method. Associations with an asterisk (\*) were identified  
965 considering a false discovery rate of 5%. NES: normalized enrichment score; ODI: oxygen  
966 desaturation index; T90: percentage of time with oxygen saturation < 90%.

967

968

969 **Table 1.** Participants' characteristics by obstructive sleep apnea (OSA) severity groups.

970 **caption:** Continuous variables presented as median [interquartile range] and categorical

971 variables presented as absolute numbers (%). AHI: apnea-hypopnea index; BMI: Body mass

972 index; DBP: diastolic blood pressure; ESS: Epworth sleepiness scale; HbA1c: glycated

973 hemoglobin; med.: medication; ODI: oxygen desaturation index; PPI: proton-pump inhibitors;

974 SBP: systolic blood pressure; T90: percentage of time with oxygen saturation < 90%; WHR:

975 waist-hip-ratio. <sup>a</sup> Percentages do not add to 100% as participants with incomplete compulsory

976 education were not included in the table.

977

978 **Supplementary Figures captions**

979 **Figure S1.** Study flowchart for the 4,839 SCAPIS-Uppsala participants with available data on

980 their gut microbiota composition.

981

982 **Figure S2.** Directed acyclic graph depicting the causal assumptions on the effect of obstructive

983 sleep apnea (OSA) on the gut microbiota composition. A directed edge (or “arrow”) from one

984 node to another represents a direct effect between these two nodes. Green line: causal path; pink

985 line: biasing path; pink nodes: ancestor of exposure and outcome; and blue nodes: ancestor of  
986 outcome.

987

988 **Figure S3.** Directed acyclic graph depicting the causal assumptions on the effect of gut  
989 microbiota on blood pressure measurements and insulin resistance. A directed edge (or “arrow”)  
990 from one node to another represents a direct effect between these two nodes. Green line: causal  
991 path; pink line: biasing path; pink nodes: ancestor of exposure and outcome; and blue nodes:  
992 ancestor of outcome.

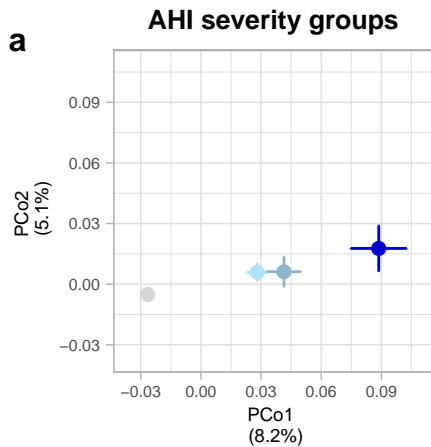
993

994 Table 1.

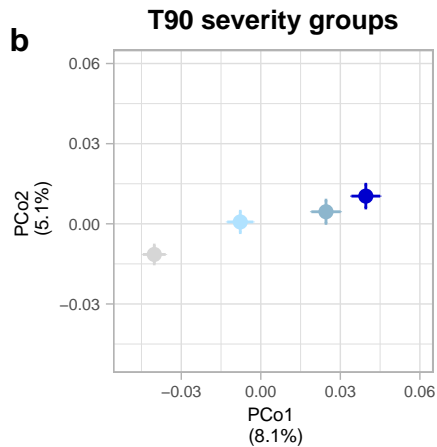
	All	No OSA (AHI < 5/h)	Mild (AHI 5–14.9/h)	Moderate (AHI 15–29.9/h)	Severe (AHI ≥ 30/h)
N	3,175	1,851 (58.3%)	899 (28.3%)	295 (9.3%)	130 (4.1%)
Age (years)	57.7 [53.9;61.4]	56.8 [53.2;61.0]	58.8 [54.9;62.0]	59.4 [55.7;62.5]	59.5 [55.5;61.7]
Female	1,708 (53.8%)	1,122 (60.6%)	446 (49.6%)	98 (33.2%)	42 (32.3%)
AHI (events/h)	3.8 [1.5;8.6]	1.7 [0.9;3.1]	7.8 [6.2;10.4]	20.1 [17.2;24.1]	38.0 [33.8;49.4]
ODI (events/h)	4.1 [1.7;9.2]	2.1 [1.0;3.6]	8.3 [6.0;11.0]	19.1 [15.3;23.7]	35.5 [29.2;42.6]
T90 (%)	2.0 [0.0;12.0]	1.0 [0.0;4.0]	5.0 [2.0;18.0]	12.0 [6.0;25.0]	20.0 [11.0;41.8]
BMI (kg/m <sup>2</sup> )	26.3 [24.0;29.2]	25.2 [23.1;27.7]	27.5 [25.2;30.3]	28.9 [26.1;32.2]	30.0 [27.4;34.2]
WHR	0.9 [0.9;1.0]	0.9 [0.8;1.0]	0.9 [0.9;1.0]	1.0 [0.9;1.0]	1.0 [0.9;1.0]
Shannon index	4.2 [3.9;4.4]	4.2 [4.0;4.4]	4.1 [3.8;4.4]	4.1 [3.9;4.4]	4.0 [3.6;4.2]
SBP (mmHg)	124 [114;135]	121 [112;131]	127 [116;138]	129 [118;140]	132 [120;144]
DBP (mmHg)	76 [70;84]	75 [68;81]	78 [72;85]	80 [74;88]	82 [74;88]
HbA1c (mmol/mol)	35 [33;38]	35 [33;37]	36 [34;38]	36 [34;39]	38 [35;41]
Hemoglobin (g/L)	141 [133;150]	139 [132;147]	142 [134;151]	146 [138;154]	146 [139;153]
Current smoker	249 (8.3%)	137 (7.8%)	79 (9.3%)	20 (7.2%)	13 (10.9%)
Alcohol intake (g/day)	5.5 [1.9;10.2]	5.2 [1.8;9.3]	6.1 [2.2;11.2]	7.2 [2.5;13.0]	6.3 [1.2;12.8]
Fiber (g/day)	18.3 [13.1;25.1]	19.2 [13.7;26.1]	17.3 [12.4;23.5]	17.5 [12.3;23.4]	16.8 [12.8;23.8]
Total energy intake (kcal/day)	1,611 [1,267;2,014]	1,624 [1,289;2,039]	1,594 [1,240;1,983]	1,593 [1,198;2,000]	1,672 [1,278;2,067]
Leisure time physical activity					
mostly sedentary	306 (10.3%)	135 (7.7%)	106 (12.6%)	41 (14.8%)	24 (19.8%)
moderate activity	1,369 (45.9%)	749 (42.8%)	425 (50.7%)	137 (49.5%)	58 (47.9%)
regular and moderate activity	964 (32.3%)	622 (35.6%)	238 (28.4%)	74 (26.7%)	30 (24.8%)
regular exercise or training	346 (11.6%)	243 (13.9%)	69 (8.2%)	25 (9.0%)	9 (7.4%)
Highest education <sup>a</sup>					
Compulsory	191 (6.3%)	82 (4.6%)	65 (7.5%)	32 (11.3%)	12 (9.9%)
Upper secondary	247 (41.0%)	681 (38.3%)	368 (42.7%)	136 (48.2%)	62 (51.2%)
University	1,593 (52.3%)	1,012 (56.9%)	421 (48.8%)	113 (40.1%)	47 (38.8%)
Birth place					
Scandinavia	2,861 (90.4%)	1,670 (90.5%)	809 (90.3%)	264 (89.5%)	118 (90.8%)
Europe	123 (3.9%)	73 (4.0%)	30 (3.3%)	15 (5.1%)	5 (3.8%)
Asia	112 (3.5%)	61 (3.3%)	37 (4.1%)	9 (3.1%)	5 (3.8%)
Other	70 (2.2%)	41 (2.2%)	20 (2.2%)	7 (2.4%)	2 (1.5%)
Type 2 diabetes	253 (8.0%)	106 (5.7%)	90 (10.0%)	28 (9.5%)	29 (22.3%)
Hypertension	674 (21.2%)	292 (15.8%)	235 (26.1%)	104 (35.3%)	43 (33.1%)
Hyperlipidemia	368 (11.6%)	169 (9.13%)	124 (13.8%)	52 (17.6%)	23 (17.7%)
Medication					
metformin	91 (2.9%)	30 (1.6%)	38 (4.2%)	9 (3.1%)	14 (10.8%)
antihypertensive med.	585 (18.4%)	244 (13.2%)	207 (23.0%)	92 (31.2%)	42 (32.3%)
hyperlipidemia med.	236 (7.4%)	92 (5.0%)	90 (10.0%)	37 (12.5%)	17 (13.1%)
PPI	94 (3.0%)	42 (2.3%)	25 (2.8%)	19 (6.4%)	8 (6.2%)
ESS	6 [3;9]	5 [3;8]	6 [3;9]	6 [4;10]	6 [4;10]



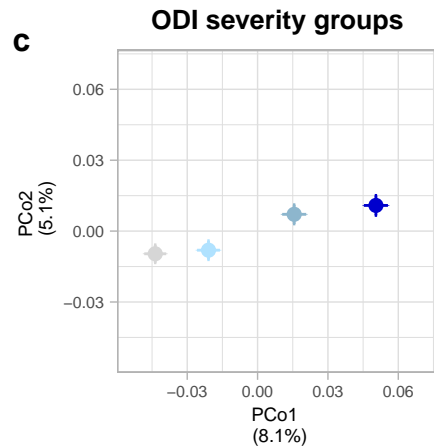
Fig. 1



- No OSA (n = 1,851)
- ◆— Mild (n = 899)
- Moderate (n = 295)
- Severe (n = 130)



- ◆— T90 = 0 (n = 1,088)
- ◆— t1 (n = 912)
- t2 (n = 759)
- t3 (n = 811)

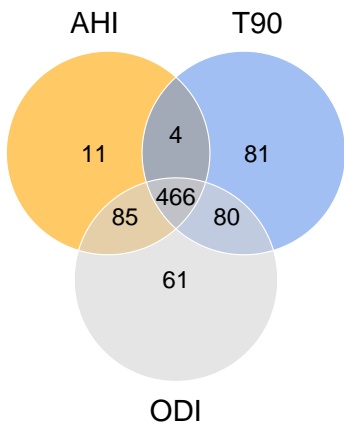


- ◆— q1 (n = 913)
- ◆— q2 (n = 885)
- q3 (n = 891)
- q4 (n = 881)

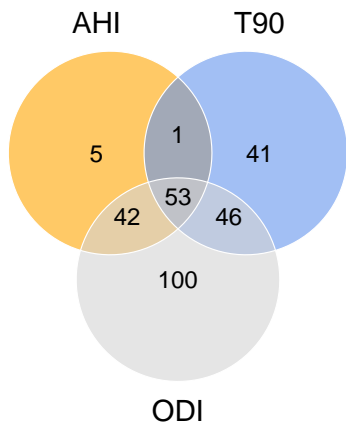


Fig. 2

**a** Not adjusted for BMI



**b** BMI adjusted



**c** Extended adjustment

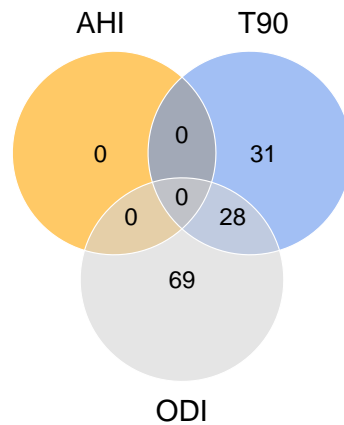


Fig. 3

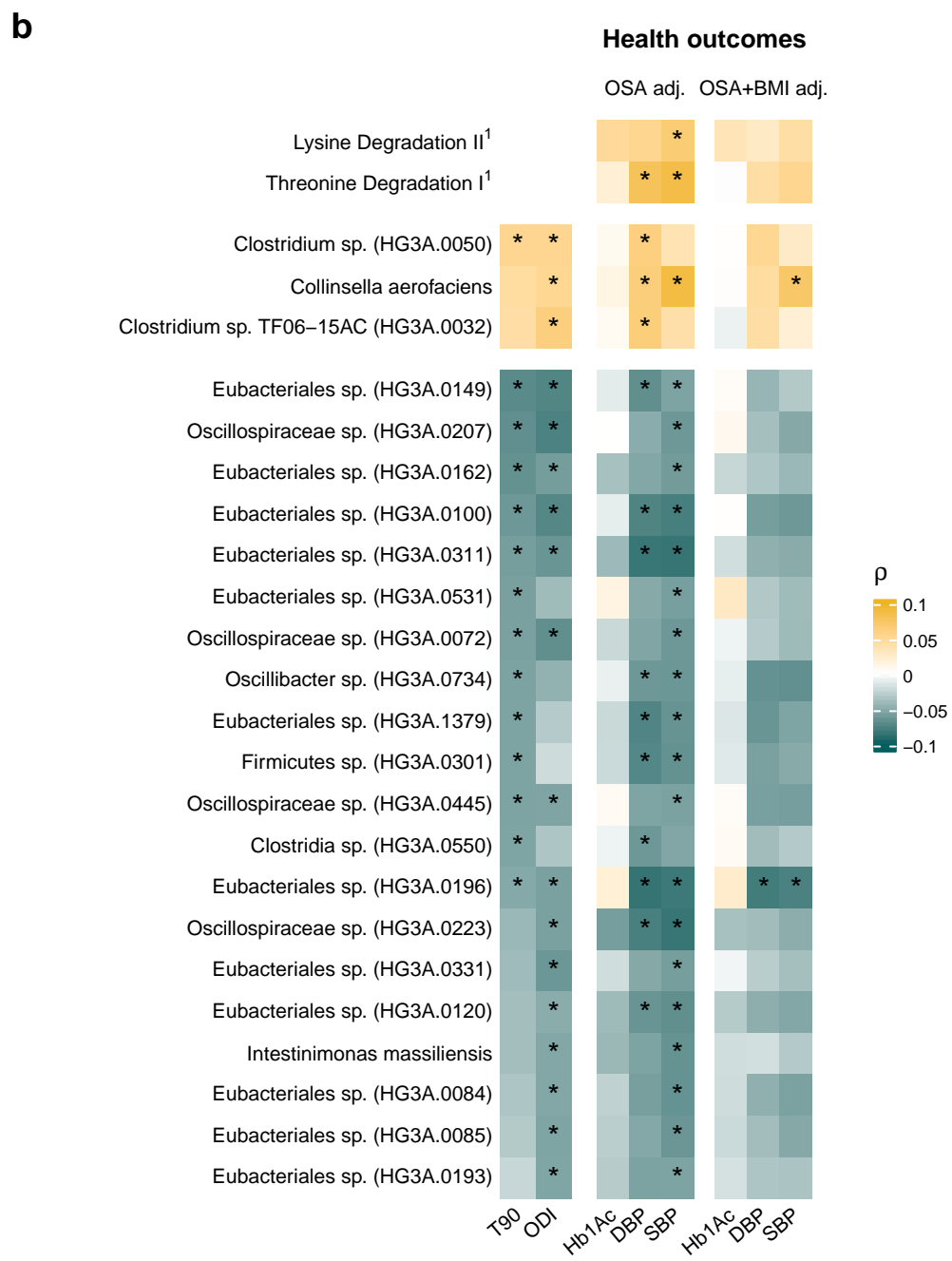
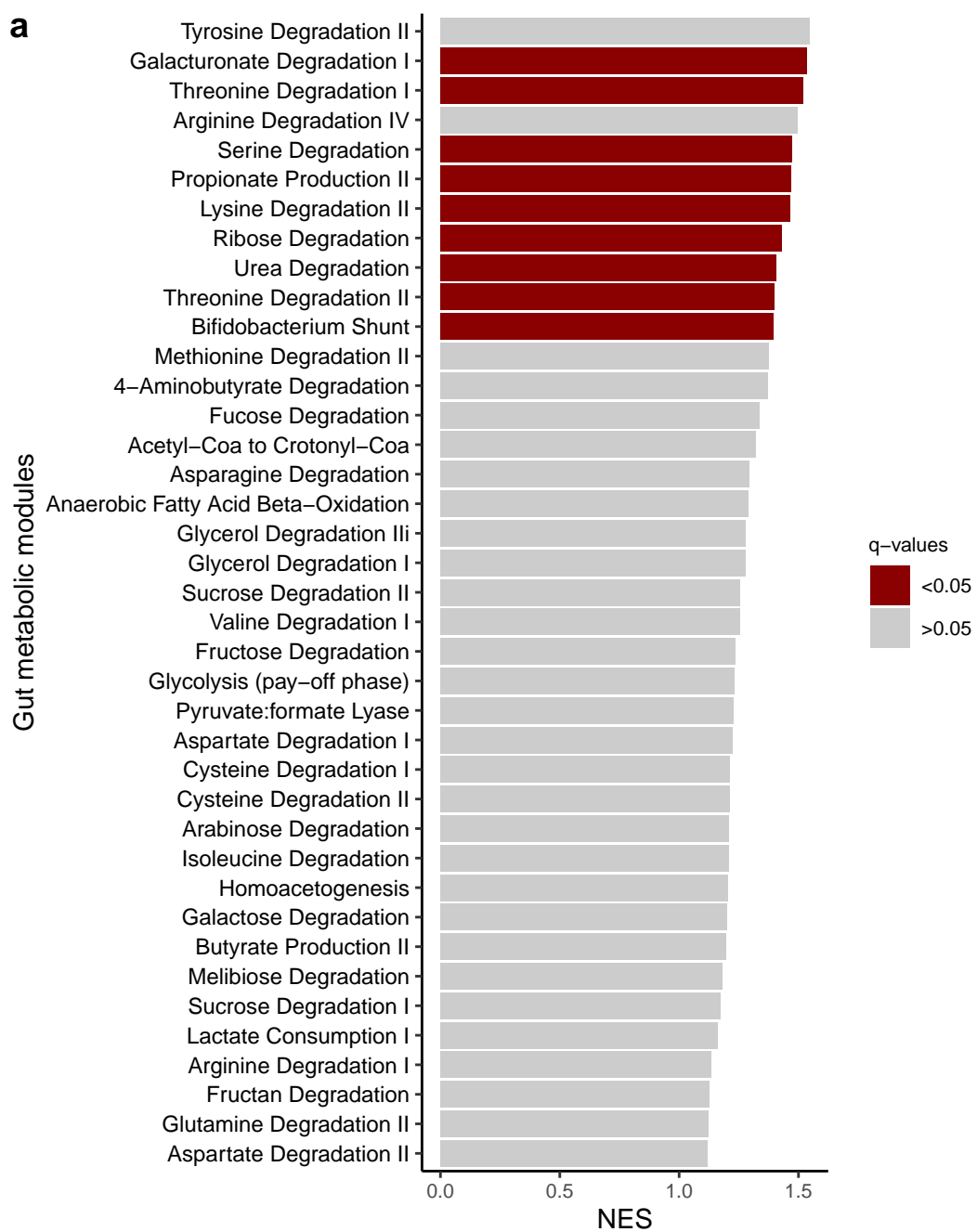
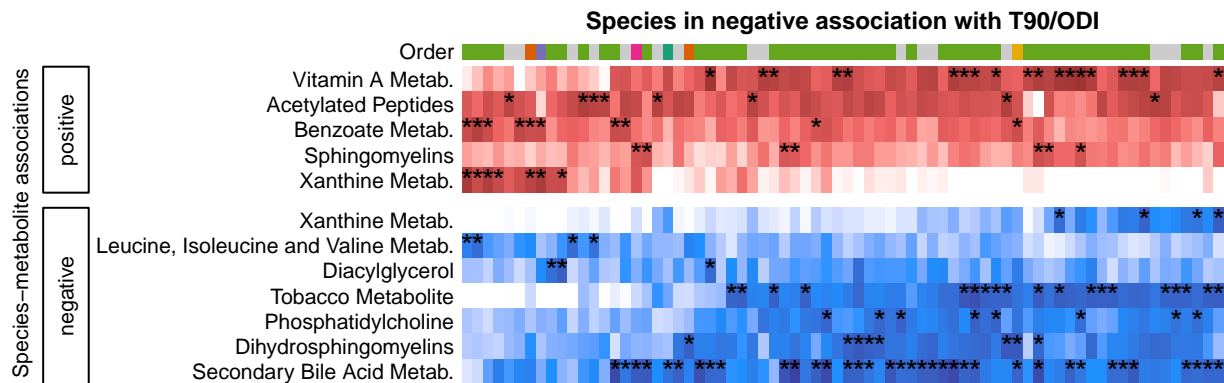


Fig. 4

**a****b**